BULLETIN DE L'ASSOCIATION MINÉRALOGIQUE DU CANADA

THE CANADIAN MINERALOGIST

JOURNAL OF THE MINERALOGICAL ASSOCIATION OF CANADA

Volume 41 February 2003 Part 1

The Canadian Mineralogist
Vol. 41, pp. 1-26 (2003)

INSIGHTS INTO ASTROPHYLLITE-GROUP MINERALS. I. NOMENCLATURE, COMPOSITION AND DEVELOPMENT OF A STANDARDIZED GENERAL FORMULA

PAULA C. PIILONEN[§] AND ANDRÉ E. LALONDE

Ottawa–Carleton Geoscience Centre, Department of Earth Sciences, University of Ottawa, Ottawa, Ontario K1N 6N5, Canada

ANDREW M. MCDONALD

Department of Earth Sciences, Laurentian University, Sudbury, Ontario P3E 2C6, Canada

ROBERT A. GAULT

Mineral Sciences Research Division, Canadian Museum of Nature, P.O. Box 3443, Station D, Ottawa, Ontario K1P 6P4, Canada

ALF OLAV LARSEN

Norsk Hydro ASA, Research Centre Porsgrunn, Porsgrunn, Norway

ABSTRACT

The composition of 135 samples of astrophyllite-group minerals from 15 localities has been established by EMPA, ICP–AES, FTIR, TGA, thermal decomposition, NRA and Mössbauer spectroscopy. A standardized general formula has been developed and is of the form $A_2BC_7D_2T_8O_{26}(OH)_4X_{0-1}$, where $^{[10]-[13]}A$ = K, Rb, Cs, H_3O^+, H_2O, Na or □; $^{[10]}B$ = Na or Ca; $^{[6]}C$ = Mn, Fe^{2+}, Fe^{3+}, Na, Mg, or Zn; $^{[6]}D$ = Ti, Nb, or Zr; $^{[4]}T$ = Si or Al, X = ϕ = F, OH, O, or □. Data acquired by Mössbauer spectroscopy, thermodynamic approximations, and EMP analyses have been used to demonstrate that F orders at the ϕ(16) site and does not occur at the two general OH sites within the *O* sheet. On this basis, formulas of the eight species of astrophyllite-group minerals have been redefined. Results from Mössbauer spectroscopy indicate Fe^{3+}/Fe_{tot} values in the range from 0.01 to 0.21, corresponding to 0.05 to 0.56 *apfu* Fe^{3+}, confirming that Fe^{2+} is the dominant valence state for iron in the structure. Minerals from silica-oversaturated and -undersaturated alkaline intrusions are distinct in chemical composition. In oversaturated rocks, the dominant member of the group is astrophyllite *sensu stricto*, which occurs as a late-stage postmagmatic phase, enriched in Rb, Fe^{2+}, Ti, Si and F. In contrast, undersaturated intrusions, in particular Mont Saint-Hilaire, Quebec, show the greatest diversity in species and range in chemical composition. Kupletskite-subgroup samples are enriched in Na, Mn, Fe^{3+}, Zn, Zr and Nb, whereas astrophyllite-subgroup samples are enriched in K, Ca, Fe^{2+}, Ti, Zr and Al. Enrichment of kupletskite-subgroup samples in Fe^{3+}, Mn and Nb suggests crystallization under more oxidizing conditions than those of the astrophyllite subgroup. Incorporation of Nb into the

§ *Current address*: Mineral Sciences Research Division, Canadian Museum of Nature, P.O. Box 3443, Station D, Ottawa, Ontario K1P 6P4, Canada. *E-mail address*: ppiilonen@mus-nature.ca

structure and the formation of Nb-bearing kupletskite and niobokupletskite are the result of the substitution $M(1)^{2+} + M(2,3)^{2+} + (Zr,Ti) + F \Leftrightarrow {}^{M(1)}Na + {}^{M(2,3)}Fe^{3+} + Nb + O$.

Keywords: astrophyllite-group minerals, kupletskite subgroup, astrophyllite subgroup, structural formula, crystal chemistry.

Sommaire

Nous avons établi la composition de 135 échantillons de minéraux du groupe de l'astrophyllite provenant de 151 endroits au moyen de la microsonde électronique, des analyses ICP–AES, spectrométrie infra-rouge avec transformation de Fourier, analyse thermogravimétrique, décomposition thermique, analyse par réactions nucléaires, et spectroscopie de Mössbauer. Nous proposons une formule générale standardisée, $A_2BC_7D_2T_8O_{26}(OH)_4X_{0-1}$, dans laquelle $^{[10]-[13]}A$ = K, Rb, Cs, H_3O^+, H_2O, Na ou □; $^{[10]}B$ = Na ou Ca; $^{[6]}C$ = Mn, Fe^{2+}, Fe^{3+}, Na, Mg, ou Zn; $^{[6]}D$ = Ti, Nb, ou Zr; $^{[4]}T$ = Si ou Al, X = ϕ = F, OH, O, ou □. Les données acquises par spectroscopie de Mössbauer, approximations thermodynamiques, et analyses à la microsonde électronique ont servi à démontrer que le F est ordonné au site ϕ(16) mais non aux deux sites OH au sein du feuillet d'octaèdres. Ainsi, nous redéfinissons la formule des huit espèces de minéraux du groupe de l'astrophyllite. Les résultats obtenus par spectroscopie de Mössbauer indiquent des valeurs Fe^{3+}/Fe_{tot} entre 0.01 et 0.21, ou bien entre 0.05 et 0.56 atomes de Fe^{3+} par unité formulaire, confirmant ainsi que le Fe^{2+} est prédominant dans la structure. Les minéraux provenant de complexes ignés sursaturés et sous-saturés en silice sont distincts en composition chimique. Dans les roches sursaturées, le membre dominant du groupe est l'astrophyllite *sensu stricto*, qui se présente comme phase tardive post-magmatique, enrichie en Rb, Fe^{2+}, Ti, Si et F. En revanche, les complexes intrusifs sous-saturés, et en particulier le Mont Saint-Hilaire, Québec, fait preuve d'une plus grande diversité dans les espèces et dans leur variabilité en composition chimique. Les échantillons du sous-groupe de la kupletskite sont enrichis en Na, Mn, Fe^{3+}, Zn, Zr et Nb, tandis que les échantillons du sous-groupe de l'astrophyllite sont enrichis en K, Ca, Fe^{2+}, Ti, Zr et Al. L'enrichissement des minéraux du sous-groupe de la kupletskite en Fe^{3+}, Mn et Nb découlerait d'une cristallisation sous conditions plus oxydantes que dans le cas des minéraux du sous-groupe de l'astrophyllite. L'incorporation du Nb dans la structure et la formation de la kupletskite niobifère ou bien de la niobokupletskite résultent de la substitution $M(1)^{2+} + M(2,3)^{2+} + (Zr,Ti) + F \Leftrightarrow {}^{M(1)}Na + {}^{M(2,3)}Fe^{3+} + Nb + O$.

(Traduit par la Rédaction)

Mots-clés: minéraux du groupe de l'astrophyllite, sous-groupe de la kupletskite, sous-groupe de l'astrophyllite, formule structurale, chimie cristalline.

Introduction

Astrophyllite *sensu stricto* is a Fe-dominant alkali titanosilicate first discovered in 1844 in a nepheline syenite pegmatite on the island of Låven, part of the Larvik complex of the Oslo Rift Valley, southeastern Norway, and later described as a "brown mica" (Weibye 1848). Astrophyllite was later named and formally described by Scheerer (1854) and Brøgger (1890). Eight species of astrophyllite-group minerals (AGM) are known; the most recently discovered, niobokupletskite, was described from Mont Saint-Hilaire (MSH; Piilonen *et al*. 2000). Astrophyllite-group minerals have been described from many alkaline intrusions, most commonly as accessory or rock-forming minerals in quartz or nepheline syenites, alkaline granites and their associated pegmatites, but also from metamorphic rocks such as nepheline syenite gneiss and riebeckite gneiss.

Although the existence of astrophyllite has been known since the late 19th century, considerable debate still exists regarding the anionic scheme, method of calculation of the general formula, and contrasts in compositional trends between over- and undersaturated alkaline. In this paper, we present the results of an extensive study on the chemical variations observed in astrophyllite-group minerals from a large number of over- and undersaturated alkaline intrusions (Table 1). Our main objectives are to (1) establish a systematic crystal-chemical nomenclature for the astrophyllite group of minerals, and (2) describe the chemical variations observed, particularly with respect to Na, Mn, Fe, Zn, Mg, Ti, Zr, Nb and F, in the various parageneses and localities. This is the first in a series of papers dealing with the crystal chemistry and paragenesis of astrophyllite-group minerals; details regarding crystal-structure variations, Mössbauer spectroscopy, and paragenesis will be presented in forthcoming papers.

Background Information

Members of the astrophyllite group have been documented from a number of alkaline intrusions including, most importantly, Mont Saint-Hilaire (Quebec), Strange Lake and Seal Lake (Labrador), the Khibina and Lovozero massifs, Kola Peninsula (Russia), Ilímaussaq, Kangerdlugssuaq, Narssarssuk and the Werner Bjerge complex (Greenland), and Mount Rosa, Pikes Peak (Colorado). Following Brøgger's original description in 1890, there have been relatively few detailed crystal-chemical studies of the astrophyllite group. The crystal structure of magnesium astrophyllite was first determined by Peng & Ma (1963), and the structure of triclinic astrophyllite (*sensu stricto*) was later determined by Woodrow (1967), who described it as a layered titanosilicate with strong affinities to biotite. Until recently, most compositions reported in the literature were

done as part of larger studies on the petrogenesis of the alkaline complexes in which they occur.

Ganzeyev *et al.* (1969) were among the first researchers to specifically investigate the isomorphous substitution of alkali cations such as Rb, Cs and Li for K in the interlayer. Similarly, Chelishchev (1972) carried out the only known experimental work on astrophyllite-group minerals, examining the extent of ion exchange of K with Na, Rb and Cs in an aqueous fluid under supercritical conditions (400 to 600°C). Results indicate increasing Na-for-K substitution with increasing temperature, the high temperatures (600°C) favoring exchange of Rb and Cs for K.

Macdonald & Saunders (1973) produced the first extensive compilation of chemical data on astrophyllite-group minerals and attempted to correlate chemical composition with paragenesis. Those minerals from undersaturated rocks were found to be characterized by higher Al, Ca, Mg, Mn, OH, F, K, Na and Zr compared to those from oversaturated rocks. No attempt was made to distinguish between Mn-dominant species and Fe-dominant species, which display strongly contrasting chemical characteristics within a single petrogenetic environment.

Layne *et al.* (1982) carried out electron-microprobe analyses on astrophyllite from silica-oversaturated and -undersaturated pegmatite dikes at Bagnæsset and Kramers Island, Kangerdlugssuaq (East Greenland) and were the first to document correlations among composition, habit and paragenesis. Tabular crystals of astrophyllite from the oversaturated dike were found to be enriched in Si, Ti, Fe, K and Na relative to prismatic, acicular crystals of astrophyllite from the undersaturated dike.

Abdel-Rahman (1992) studied astrophyllite from peralkaline granites and associated metasomatized wallrocks of the Mount Gharib intrusion (Egypt) and concluded that astrophyllite is the product of a metasomatic reaction, forming at the expense of arfvedsonite.

Christiansen (1998) studied chemical variations in a suite of astrophyllite-group minerals from various localities in Greenland and carried out a single-crystal X-ray refinement on the structure of kupletskite from Kangerdlugssuaq (Christiansen *et al.* 1998).

TABLE 1. LOCALITY INFORMATION FOR SAMPLES OF ASTROPHYLLITE-GROUP MINERALS IN THIS STUDY

AFR	Zomba-Malosa, Malawi, Africa	
AFR1 (GM1998.7)		granitic pegmatite
EGY	Mount Gharib, Egypt (data from Abdel-Raman 1992)	
R1200		peralkaline granite
R3090		metasomatized wallrock, peralkaline granite
GJER	Gjerdingen intrusion, Norway	
NOR3 (RW–3)		alkali granite
GREEN	Various locations, Greenland (data from Christiansen 1999)	
CC4		granitic pegmatite, Astrophyllite Island, Kangerdlugssuaq
CC7AB		nepheline syenite pegmatite, Bagnæsset, Kangerdlugssuaq
KHIB	Khibina massif, Kola Peninsula, Russia	
RUS1		nepheline syenite pegmatite
RUS3 (CMNMI-44135)		trachytic nepheline syenite
RUS6 (CMNMI-53309)		nepheline syenite pegmatite
LAB	Letitia Lake, Mann #1, Labrador, Canada	
LAB2 (GSC-62047)		peralkaline nepheline gneiss
LANG	Langesundsfjord area, Oslo Rift Valley, Norway	
NOR1 (RW-1)		nepheline syenite pegmatite (Vesle Arøya)
NOR10 (AOL-3)		nepheline syenite pegmatite (Saga I Quarry, Morje)
NOR14 (AOL-7)		nepheline syenite pegmatite (Bratthagen, Lagendalen)
LOV	Lovozero massif, Kola Peninsula, Russia	
RUS9 (HC-1048)		nepheline syenite pegmatite (Lephke-Nelm)
LUKS	Luksefjell, Norway	
NOR21 (AOL-11)		alkali granite pegmatite
MSH	Mont Saint-Hilaire, Quebec, Canada	
MSH2 (NMNS-4)		nepheline syenite pegmatite
MSH3 (NMNS-5)		nepheline syenite pegmatite
MSH7 (NMNS-11)		nepheline syenite pegmatite
MSH10AB (NMNS-14)		nepheline syenite pegmatite
MSH18AB (NMNS-25)		altered nepheline syenite pegmatite
MSH19AB (NMNS-26)		altered nepheline syenite pegmatite
MSH20 (NMNS-27)		nepheline syenite pegmatite
MSH29 (CMNMC)		metasomatic unit
MSH31 (CMNMC-F882)		natrolite pegmatite
MSH42*		nepheline syenite pegmatite
MSH44		sodalite syenite
MSH45		sodalite syenite xenolith
POR	Point of Rocks, New Mexico, U.S.A.	
US9 (HDL)		nepheline syenite
PP	Mount Rosa, Pikes Peak, Colorado, U.S.A.	
US1 (CMNMI-44288)		granitic pegmatite

CMNMC/CMNMI/NMNS: Canadian Museum of Nature collection, GSC: Geological Survey of Canada collection, GM: Geological Museum, Copenhagen, RW: R. Werner collection, CC: C.C. Christiansen collection, AOL: A.O. Larsen collection, HC: L. Horváth collection, HDL: H. DeLinde collection. * Holotype niobokupletskite.

Analytical Methods

Electron-microprobe analyses

A total of 659 electron-microprobe analyses (EMPA) were done on a JEOL 733 electron microprobe, operating in wavelength-dispersion mode, using Tracor Northern 5500 and 5600 automation software. The operating conditions were as follows: beam diameter 20 μm, operating voltage 15 kV, and beam current 20 nA. Data reduction was performed using a PAP routine in XMAQNT (C. Davidson, CSIRO, pers. commun.). A total of 24 elements were sought, and the following standards were employed: sodic amphibole (Na$K\alpha$, Si$K\alpha$), sanidine (K$K\alpha$, Al$K\alpha$), diopside (Ca$K\alpha$, Mg$K\alpha$), tephroite (Mn$K\alpha$), almandine (Fe$K\alpha$), rutile (Ti$K\alpha$), synthetic $MnNb_2O_6$ (Nb$L\alpha$), vlasovite (Zr$L\alpha$), zincite (Zn$L\alpha$), phlogopite (F$K\alpha$), pollucite (Cs$L\alpha$), celestine (Sr$L\alpha$), sanbornite (Ba$L\alpha$), rubicline (Rb$L\alpha$), synthetic $NiTa_2O_6$ (Ta$M\alpha$), and hafnon (Hf$M\alpha$). Count times for all elements were 25 seconds or 0.5% precision, whichever was obtained first, except for Cs and Rb (100 s), and Hf (50 s). Overlap corrections for Si($K\alpha$)–Sr($L\alpha$), Zr($L\beta$)–Nb($L\alpha$) and Mn($K\beta$)–Nb($L\alpha$) were performed. Also sought but not detected were Cl, La, Ce, Yb, P, Th, Pb, Ni, V, U, W, Sc, S and Mo.

Many of the crystals, in particular those from Mont Saint-Hilaire, show extensive chemical zoning, as viewed in back-scattered electron images. An attempt was made to establish the composition of all zones at a

scale of >20 μm. It was not possible to analyze smaller zones owing to constraints on the beam diameter; analyses performed with a beam diameter <20 μm resulted in extensive volatilization of the sample.

The effects of electron-beam diameter used in the analyses

During the course of the study, we obtained low analytical totals (≈ 96 to 98 wt.%) with a standard defocused beam 20 μm in diameter. We suspected that migration of light elements (*e.g.*, Na and Si) might be responsible. Beam-induced heating and charging effects are common in minerals, their synthetic analogues and glasses, particularly in K- and Na-bearing silicates (Nielsen & Sigurdsson 1981, Spray & Rae 1995). We investigated the time-dependent decomposition of astrophyllite-group minerals at a fixed diameter of the beam.

Two separate samples were chosen for analysis on the basis of chemical homogeneity and lack of inclusions: NOR3 and RUS1. The three elements most likely to undergo volatilization or migration, Si, Na, and K, were monitored at three-second intervals for a total of 105 s (Fig. 1). Volatilization of these elements during the specified time-period and at the operating conditions

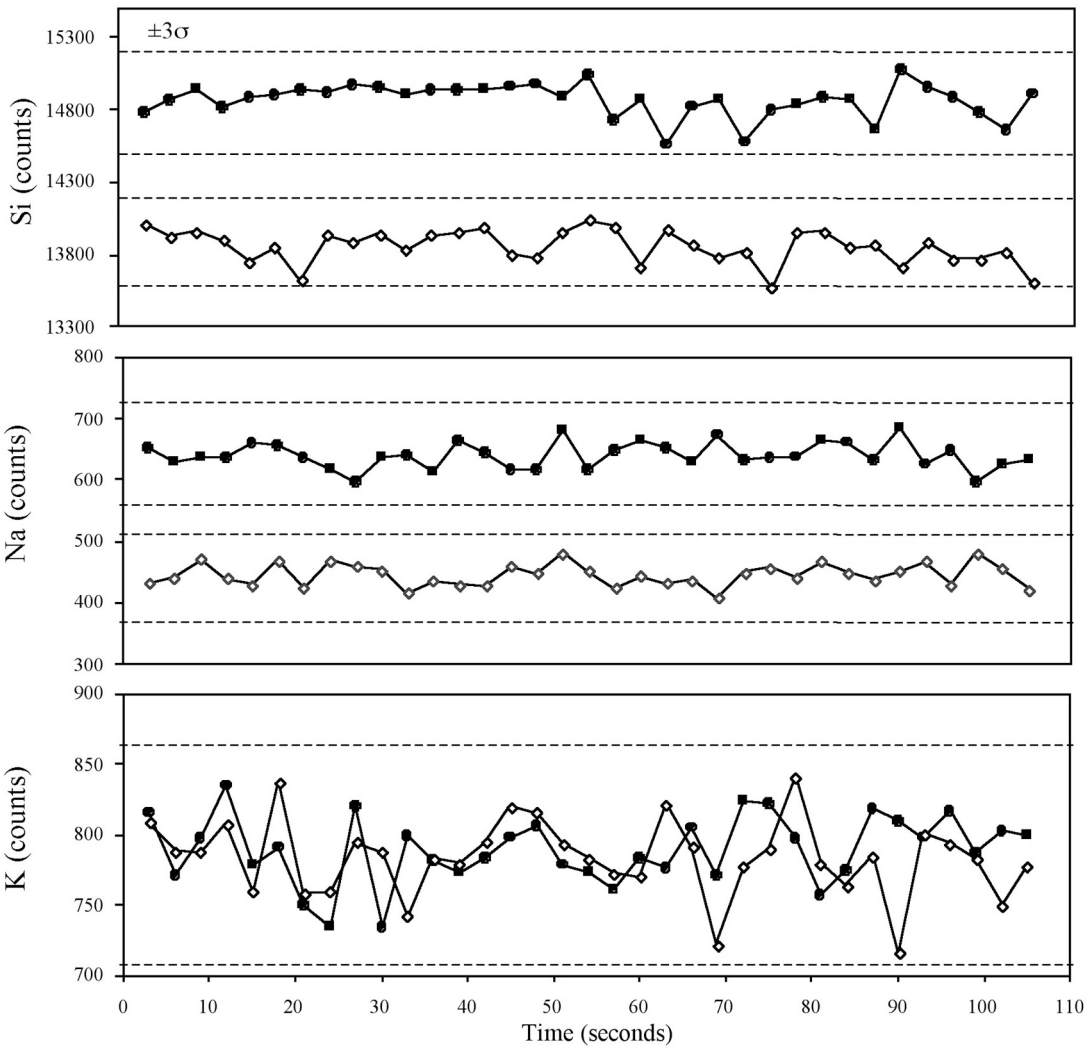

FIG. 1. Intensities of the $K\alpha_1$ line of Si, Na and K as a function of time taken for analysis of kupletskite (closed circles) and astrophyllite (open diamonds). Dashed lines indicate ±3σ for each sample.

specified is insignificant at the 3σ level and can therefore be ruled out as a potential cause of low analytical totals. Previous work on astrophyllite-group minerals (T.S. Ercit, pers. commun.) using both a point-focused (1 μm) and a 20 μm defocused beam over a period of 360 s indicates loss of Si, Na and K only with the point-focused beam.

Although analytical totals for the majority of our samples range from 95 to 98%, the resultant sums of the cations are excellent (~19.85 to 20.00 *apfu*), which suggests that the low totals are not entirely the result of errors in the experimentally determined $Na_2O + K_2O$ contents, or that instrument calibration was inadequate. Rather, the counts for all the elements monitored are depressed. The cause of the low totals is therefore likely due to a combination of factors that may or may not include: (1) selection of standards, (2) differing conditions of carbon coating of samples and standards, (3) micrometric scratches and abrasion of the grains during polishing, (4) sample charging, (5) the presence of undetected constituents other than H_2O, (6) the presence of errors in the astrophyllite structure due to polysomatism, or (7) the presence of undetected structural or adsorbed H_2O, either on the surface or in the interior of the crystals.

We conclude that the last factor is the largest contributor to the low totals; interpretation of Fourier-transform infrared (FTIR) spectra and thermal gravitational analysis (TGA) has confirmed the presence of adsorbed H_2O in all samples (~0.2 wt.%). Analysis of such grains by EMPA will result in analytical totals less than ideal, but as the adsorbed H_2O is not structural, calculations of empirical formulas will still yield excellent sums of cations.

ICP–AES analyses for Li

A suite of 15 samples from MSH were analyzed for Li using inductively coupled plasma – atomic emission spectroscopy (ICP–AES). Samples were ground in a mortar and pestle, weighed (range: 6.1 to 81.0 mg depending on availability of material), and rinsed with deionized water. Digestions were done as follows: 5 mL of hydrofluoric acid was added to each sample, and the mixture allowed to digest for one hour at room temperature (RT). Nitric acid (2 mL) and perchloric acid (1 mL) were then added to the solution and allowed to further digest for 24 hours (RT). An additional 5 mL of hydrofluoric acid, 2 mL nitric acid, and 1 mL perchloric acid were added to the solution and left to further digest the residue for one hour on a hot plate until all the liquid had evaporated. The final residue was mixed with 3 mL hydrochloric acid in a volumetric flask and filled to 25 mL with deionized water. Three standards were used during the analysis procedure: SY–3 (syenite rock, 92 ppm Li), MRG–1 (Mount Royal gabbro, 4.2 ppm Li) and Mica–Fe (1200 ppm Li). Lithium contents in the samples studied range from 42.7 to 453.3 ppm.

Fourier-transform infrared spectroscopy

Fourier-transform infrared (FTIR) spectroscopy was done on selected samples in order to evaluate the presence of OH^- and to ascertain the presence of species such as H_2O or CO_3^{2-}. Samples were hand-picked under the binocular microscope and then ground under acetone in a mortar and pestle to a coarse powder (~20 μm). All analyses were performed on a Bomem Michelson MB–100 Fourier transform infrared spectrometer equipped with a mercury cadmium telluride (MCT) detector at the Canadian Conservation Institute (Ottawa, Canada). A small mass of powder was mounted in a diamond-anvil microsample cell, and pressure was applied to crush the sample further. The diamond cell was then positioned in the microbeam chamber of the spectrometer. A room-temperature spectrum was collected from 4000 to 400 cm^{-1} using the spectrum of the empty diamond anvil cell collected with the same parameters as a reference.

The absorbance spectra of all astrophyllite-group minerals examined show broad peaks in the high-frequency range (4000 to 1000 cm^{-1}) attributable to O–H stretching (~3600 cm^{-1} and an associated shoulder centered at ~3300 cm^{-1}), adsorbed H_2O (~3400 cm^{-1}), and a weak peak at ~1650 cm^{-1} attributable to H-O-H bending of absorbed or molecular H_2O (Farmer 1974). Some of the spectra show a small peak at 1900 cm^{-1}, which may be attributed to molecular H_2O. The middle- to lower-frequency end of the spectrum (1000 to 400 cm^{-1}) is characterized by symmetric Si–O stretching (~1000 cm^{-1}) and bending (~690 and 650 cm^{-1}) bonds. The two samples of niobokupletskite (MSH10B and MSH42) show one asymmetric Si–O stretching band (~965 cm^{-1}), whereas samples that are Ti-dominant have two prominent Si–O stretching bands (~1050 and 960 cm^{-1}). Low-frequency bands between 400 and 450 cm^{-1} can be attributed to (Mn,Fe)–O stretching (Farmer 1974). Infrared spectra for a suite of representative samples are shown in Figure 2.

Nuclear reaction analysis

Nuclear reaction analysis (NRA) is a technique that has the ability to accurately determine hydrogen contents in solids with a sensitivity on the order of 10 ppm. Nuclear reaction analysis employs MeV ion beams to induce nuclear reactions in solid materials (Cohen *et al.* 1972). The most common ion beam used for hydrogen determination is ^{15}N, using the reaction:

$$^{15}N + {}^{1}H \Rightarrow {}^{4}He + \gamma\text{-ray} \quad (1).$$

A beam of ^{15}N ions is used to bombard the sample, placed under vacuum, and the number of characteristic γ-rays produced (*i.e.*, those that achieve resonance of 6.385 MeV) is measured. The γ-rays are detected by a scintillation detector located approximately 2 cm behind

the sample. The number of γ-rays produced is directly proportional to the number of H atoms on the surface of the sample. Conversion of raw counts to H contents (H/cm^2) is given by

$$\text{H content} = KY - E/-x \quad (2)$$

where Y is the γ-ray yield (counts/concentration of incident ions), K is an experimental constant independent of the material being analyzed, and $-E/-x$ is the energy loss of the incident beam of ions (Lanford 1992). Increasing the energy of the beam allows for analysis of the sample at depth, such that as the higher-energy beam loses energy through surface-level collisions, resonance can only occur at increasing depth. In this way, depth profiling of H can be accomplished (Lanford 1992) and care taken to avoid analyzing for surface H_2O. For the purpose of determining H contents in astrophyllite-group minerals, an average H content was measured assuming an average density of 3.2 g/cm^3.

Results from NRA give a range of 4.4 to 7.4 × 10^{21} H/cm^3, corresponding to 3.1 to 5.0 H *apfu*, respectively. The range in H contents can be primarily explained by the two anion substitutions $F^- \Leftrightarrow OH^-$ and $F^- \Leftrightarrow O^{2-}$, and the chemical heterogeneity that is inherent in the samples studied.

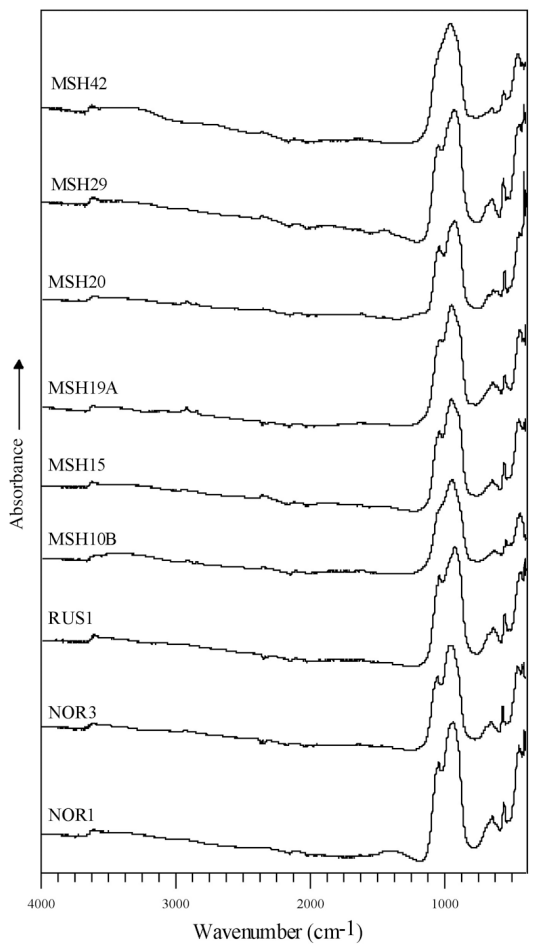

FIG. 2. FTIR absorbance spectra of representative astrophyllite-group of minerals.

Thermal decomposition and thermal gravitational analyses

Five samples were studied by a combination of thermal decomposition and thermal gravitational analyses (TGA). Thermal decomposition analysis were performed on a LECO RC–412 multiphase analyzer using 0.07 to 0.12 g of sample material. Samples were heated in an oxygen combustion chamber to 1000°C, and the quantity of expelled H_2O was detected using an IR spectrometer and calibrated using known standards. The range of measured H_2O contents given by thermal decomposition is 3.55 to 3.99 ± 0.1 wt.% H_2O, approximately 1 to 1.5 wt.% higher than calculated H_2O values. Thermal gravitational analysis of the same samples indicated that ~0.2 wt.% H_2O is given off below 105°C, whereas the majority of the H_2O was lost between 120° and 850°C. The gradual loss of H_2O over a wide range of temperatures indicates that bond strengths to the H_2O groups are quite variable, suggesting that the H_2O may be adsorbed on surfaces or weakly bonded in the interlayer. The small component of molecular H_2O (1 to 1.5 wt.%) does not seem to be important on a structural level and was not detectable during single-crystal *X*-ray structure refinements.

Mössbauer spectroscopy

Calculation of Fe^{2+}/Fe^{3+} in astrophyllite-group minerals is complicated by the wide range of both cation and anion contents observed, as well as the presence of vacancies in the structure. Until recently, Fe^{3+} was considered to be a minor component in these minerals, a conclusion based primarily on wet-chemical determinations (Macdonald & Saunders 1973) and charge-balance calculations. Mössbauer spectroscopy was used in an effort to determine Fe^{2+}/Fe^{3+}, and to provide information on the coordination number of both Fe^{2+} and Fe^{3+} in the astrophyllite structure, and on variations in the local electronic environment around the Fe cations.

Samples studied by Mössbauer spectroscopy have Mn# [Mn/(Mn + Fe_{tot})] values in the range from 0.10 to 0.81. Whereas there is wide variation in chemical composition among the samples, the Mössbauer spectra of all minerals examined are remarkably similar. The spectra display two strong absorption peaks centered at ~–0.1 and 2.3 mm/s and a third, weaker shoulder at

~0.9 mm/s. These peaks correspond, respectively, to (1) the sum of the low-energy lines from $^{[6]}Fe^{2+}$ and $^{[6]}Fe^{3+}$ doublets, (2) the high-energy lines from $^{[6]}Fe^{2+}$ doublets, and (3) the high-energy lines from $^{[6]}Fe^{3+}$ doublets. Manning (1969) performed an optical spectroscopic study of a sample of astrophyllite from St. Peter's Dome (Colorado) and suggested that the observed pleochroism is the result of Ti^{3+}–Ti^{4+} intervalence electron transfer, rather than electron transfer between Fe^{2+} and Fe^{3+}. The lack of an absorption band at ~14,000 cm^{-1}, corresponding to an Fe^{2+}–Fe^{3+} electron transfer, suggested that the two cations are not located in the same sheet and, as such, Manning (1969) proposed a $Fe^{3+} \Leftrightarrow Ti^{4+}$ substitution in *D*. Results from the Mössbauer spectroscopic study indicates that Fe^{3+} is restricted to the *O* sheet (*C*) and does not substitute for the high-field-strength elements (HFSE) in *D*. Furthermore, $^{[4]}Fe^{3+}$ does not appear to play a role in the astrophyllite structure; the characteristic $^{[4]}Fe^{3+}$ contribution in mica spectra, occurring at ~0.4 to 0.5 mm/s (Rancourt *et al*. 1992, Lalonde *et al*. 1996), is not observed in any of our spectra.

Overview of the Structure

The structure of astrophyllite-group minerals (Figs. 3a, b) can be considered as two composite sheets stacked along [001] in a 2:1 ratio. The first is a sheet of octahedra (*O* sheet) extending from $z \approx 0.40$ to 0.60 in triclinic species and from $z \approx -0.05$ to 0.05 in monoclinic species (kupletskite), which consists of a closest-packed sheet of MO_6 octahedra (where *M* may represent Mn, Fe^{2+}, Fe^{3+}, Mg or Na). There are four crystallographically distinct sites, designated *M*(1) through *M*(4). The *O* sheet is sandwiched between two *H* sheets, extending from $z \approx -0.15$ to -0.05. The *H* sheets consist of open-branched *zweier* [100] single chains of $[Si_4O_{12}]^{8-}$ (Liebau 1985), which are in turn cross-linked by corner-sharing $D\phi_6$ octahedra [ϕ: unspecified anion], or DO_5 polyhedra as in magnesium astrophyllite (Shi *et al*. 1998), where *D* represents Nb, Ti, and Zr. The resultant Si:*D* ratio is 4:1. Individual $D\phi_6$ octahedra are linked across the interlayer space *via* $\phi(16)$. The interlayer space contains two crystallographically distinct cation sites, *A* and *B*, which are host to [11]- to [13]-coordinated K + Na and [10]-coordinated Na, respectively.

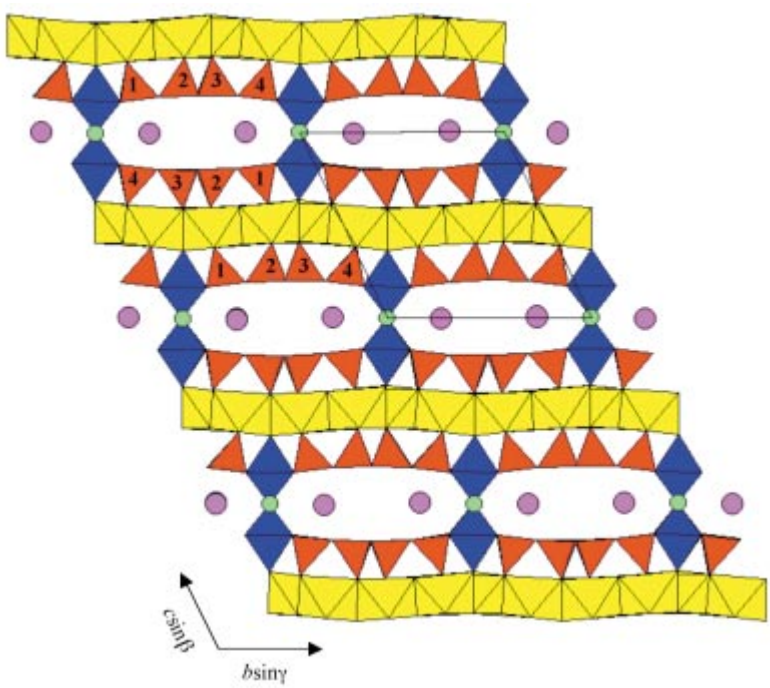

FIG. 3a. Crystal structure of triclinic astrophyllite-group mineral ($P\bar{1}$) projected down [100] (unit cell outlined). *O* sheet: yellow, *D*: blue, *T*: red, *A*: magenta, *B*: green. The four *T* sites are indicated to show symmetry across the interlayer.

Nomenclature of the Astrophyllite Group and Standardized General Formula

Previous work

There has been little consensus among researchers regarding the correct general formula to be used for astrophyllite-group minerals. In fact, some investigators have considered these minerals to be non-stoichiometric owing to the presence of vacancies and cation sums regularly less than the ideal 20.00 *apfu*. The problem with defining a general formula relates to a combination of slightly non-stoichiometric compositions exhibited by most samples (*i.e.*, vacancies in the interlayer and a variable composition at the anion site), a lack of complete and accurate chemical data, and a lack of in-depth single-crystal X-ray refinements of the structure of members of the group. The general formula currently accepted by most researchers is $A_3B_7C_2D_8X_{31}$, with formulae typically being calculated based on 31(O + OH + F). However, a number of ideal anion compositions have been proposed including X = 31(O,OH,F) (Woodrow 1967, Nickel *et al*. 1964), 30O (Layne *et al.* 1982), 27O and 4(OH,F) (Kapustin 1973), 26O and 5(OH,F) (Macdonald & Saunders 1973, Martin 1975, Abdel-Rahman 1992), 24O and 7(OH,F) (Layne *et al*. 1982), 26O, 4(OH) and F (Christiansen *et al*. 1998), and 26O and 4(OH,F) (Shi *et al.* 1998).

The most commonly accepted scheme used to calculate empirical formulae is 24O and 7(OH,F). This scheme may have been used to compensate for the characteristically low analytical totals exhibited by most astrophyllite-group minerals; specifically, calculation of formulae on the basis of 7(OH,F) results in sums that are ~2 wt.% higher relative to those calculated with 5(OH,F) (*i.e.*, ~100 wt.% *versus* 96–98 wt.%, respectively). However, resultant cation totals are deficient by as much as 0.50 atoms per formula unit (*apfu*; *i.e.*, $\Sigma_{cations} < 20.00$ *apfu*).

Results of the current study: anionic scheme and the ϕ(16) site

Previously, direct measurement of the volatile contents in these minerals, in particular H_2O, have been limited to TGA (Martin 1975) and wet-chemical analyses (Macdonald & Saunders 1973). In order to establish the anion composition of minerals of the astrophyllite group, selected samples were analyzed by FTIR, NRA, TGA and thermal decomposition. In addition, bond-valence sum (BVS) calculations were done using data obtained from single-crystal X-ray refinements of the structure (Piilonen *et al*. 2003).

Single-crystal X-ray structure refinements and bond-valence calculations of 19 triclinic samples and of kupletskite-*Ma2b2c* (Piilonen *et al.* 2003) indicate the presence of 13 sites in general positions occupied by divalent anions (BVS range: 1.842 to 2.140 *vu*), two sites in general positions occupied by monovalent anions [O(4) and O(5), BVS range: 0.985 to 1.177 *vu*], and a mixed-valence site, ϕ(16) (BVS range: 1.105 to 1.86 *vu*). The corresponding anionic scheme, based solely on results from single-crystal X-ray refinements of the structure, is $O_{26}(OH,F,O)_5$.

The occupancy of the two monovalent anion sites in the *O* sheet [O(4) and O(5)] and questions related to the mixed valence ϕ(16) site have been the subject of debate in past studies, the focus of which concerns the degree of ordering of OH and F over these three sites. It has been previously suggested that F orders preferentially at the ϕ(16) site and does not substitute for OH in the *O* sheet (Christiansen *et al.* 1998). This inference is based on the fact that F contents in all astrophyllite-group minerals (both from this study and in the literature) exhibit a limited range, from below the detection limit to one *apfu*, suggesting a single site for F. Owing to their similarity in scattering powers (Mo$K\alpha$ radiation), site refinement involving F^- and O^{2-} could not be performed. However, bond-valence sums for O(4) and O(5) range from 0.985 to 1.177 *vu* (average: 1.089 *vu*), whereas for ϕ(16), they range from 1.105 to 1.86 *vu* (average: 1.293 *vu*), suggesting monovalent anions only in O(4) and O(5) and a mixed valence in ϕ(16). Further evidence, including Mössbauer spectroscopy, thermodynamic estimates of ΔG_{rxn} for F compounds, and results from EMPA, are presented to resolve the issue of ordering of OH, F and O.

Mössbauer spectroscopic studies of synthetic micas along the annite–fluorannite join have shown the F content to be negatively correlated with the average quadrupole splitting (<QS>; Fig. 4; Rancourt *et al.* 1996). In these micas, the variations observed in the quadrupole splitting distributions (QSD) are due to local distortions imposed on the $Fe\phi_6$ octahedron, the result of OH ⇔ F substitution, and the formation of local FeO_4F_2, $FeO_4(OH)F$ and $FeO_4(OH)_2$ configurations. The negative trend between <QS> and F content is also observed in biotite from granites (Shabani 1999; Fig. 4), although not as well developed. Mössbauer spectroscopy was done on a suite of astrophyllite-group minerals with F contents ranging from 0.15 to 0.97 *apfu*. If substitution involving F and OH was occurring in the *O* sheet [*i.e.*, O(4) and O(5)], a similar trend might be expected. However, data for these minerals (Fig. 4) plot far from the trend line defined by the OH ⇔ F substitution, suggesting that (1) F does not substitute for OH, and (2) it is not present within the *O* sheet, but is located at an anion site that does not coordinate with a Fe cation [*i.e.*, ϕ(16)].

The Fe–F avoidance principle is a well-known phenomenon in mafic silicate minerals (Mason 1992). Iron–fluorine avoidance results in significant controls on cation order in minerals containing both species owing to the greater strength of Mg–F bonds compared to Fe–F bonds. A thermodynamic approach can be used to quantify the preference of Mg over Fe for F (Munoz 1984):

$$FeF_2 + Mg(OH)_2 = Fe(OH)_2 + MgF_2 \quad (3).$$

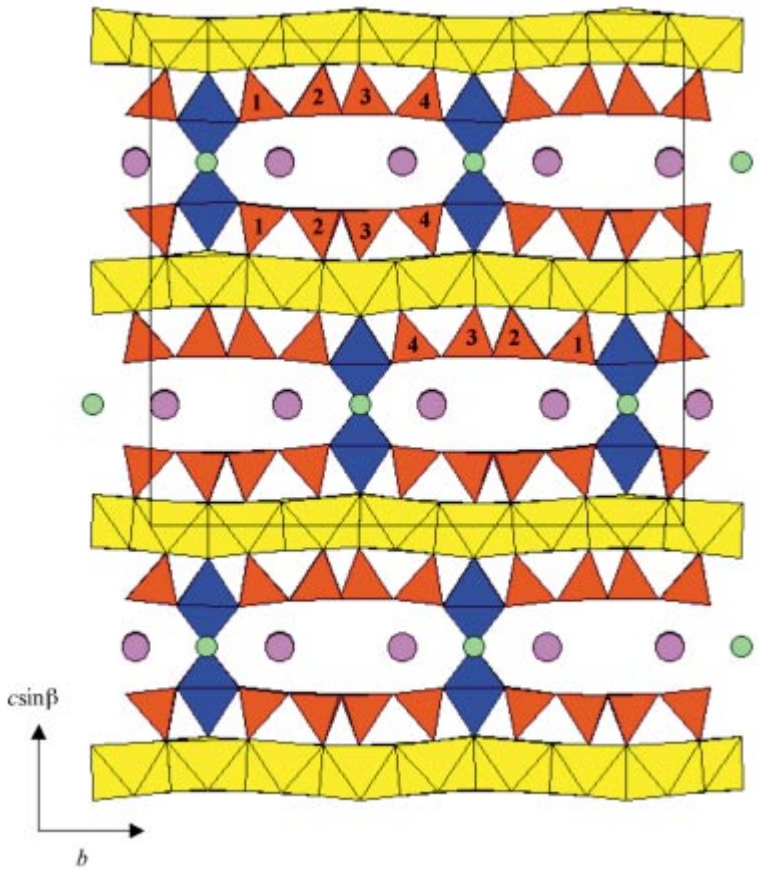

FIG. 3b. Crystal structure of kupletskite (monoclinic, *C*2/*c*) projected down [100] (unit cell outlined). *O* sheet: yellow, *D*: blue, *T*: red, K: magenta, Na: green. The four *T* sites are indicated to show symmetry across the interlayer.

The resultant ΔG_{rxn} for this exothermic reaction is –21.06 kcal (25°C), indicating that the reaction proceeds to the right and that Mg–F bonds are more likely to form. In astrophyllite-group minerals, the Mn ⇔ Fe substitution predominates, and Mg is generally not present in significant concentrations. As such, a similar approach should be applicable in evaluating the degree of Mn–F avoidance. Equilibrium values of MnF_2 were calculated using additive sums of free energies for Mn^{2+} and F (owing to the lack of experimentally derived values for complexes involving Mn). The preference of Mn and Fe for F can be calculated using:

$$FeF_2 + Mn(OH)_2 = Fe(OH)_2 + MnF_2 \quad (4).$$

The ΔG_{rxn} for (4) is –4 kcal (*i.e.*, slightly exothermic, 25°C), indicating no significant preference for Mn–F or Fe–F bonds. Experiments involving aqueous solutions with both Mn and Fe indicate that the two elements behave similarly and will generally avoid bonding with F (Munoz & Ludington 1974, Mason 1992), hence implying not only Fe–F avoidance, but Mn–F avoidance as well. The existence of Fe–F and Mn–F avoidance, coupled with the lack of a strong negative correlation between Fe–F and Mn–F, suggest that the monovalent anion sites O(4) and O(5), both of which are ligands to Mn and Fe cations within the *O* sheet, are occupied solely by OH.

Similar thermodynamic experiments involving aqueous solutions of Ti, OH and F have been conducted (McAuliffe & Barratt 1987, Mason 1992). Results indicate that Ti–F complexes can be readily synthesized, whereas those of Ti–OH are difficult to produce, suggesting a Ti–OH avoidance. This can be shown qualitatively using the equation

$$2FeF_2 + Ti(OH)_4 = 2Fe(OH)_2 + TiF_4 \quad (5)$$

calculated using additive sums of the free energies for Ti^{4+}, F^-, and OH^-. The ΔG_{rxn} for Eqn. 5 is –44 kcal (25°C), indicating a strong preference of Ti over Fe for F. A similar situation exists for Zr. Both Zr and Ti, because of their low electronegativities, form stable complexes with F except in cases where extremely high aH^+ or aCO_2 exist (Crerar *et al.* 1985, Aja *et al.* 1995). Thermodynamic and solubility calculations for various temperatures show that Zr preferentially complexes with OH over a wide range of pH conditions and temperatures, but will complex with F in F-rich and Ca-poor hydrothermal brines (Aja *et al.* 1995, Salvi & Williams-Jones 1995) with mixed hydroxyfluoride complexes [*e.g.*, $Zr(OH)_2F_2$] as the dominant species in solution (Salvi *et al*. 2000).

On the basis of data acquired by Mössbauer spectroscopy, thermodynamic approximations, and given the restricted range of F contents observed in astrophyllite-group minerals, we propose that F orders at the ϕ(16) site and does not occur at the two general OH sites within the *O* sheet. It must be emphasized here that the values of free energy used in our calculations were derived from experiments at 25°C and are (at best) only estimates for the processes that are at work in a magma or hydrothermal fluid. The lack of equilibrium conditions in such complex environments, coupled with the wide range of temperature, preclude the possibility of quantitatively using thermodynamic data based on standard conditions to predict complexing in melts. Nevertheless, the use of sums of additive free energies has been shown to give reasonable approximations for compounds for which thermodynamic data are not available (*i.e.* TiF_4, Krauskopf 1967), and therefore considered to be useful in this context as long as the qualitative aspect of the results is recognized.

The above results suggest the anionic scheme applicable to any mineral of the atrophyllite group to be $O_{26}(OH)_4(F,O,OH,\square)$. For all members except magnesium astrophyllite, the anionic scheme will be of the form $O_{26}(OH)_4(F,O,OH)$. Calculation of bond-valence sums for the anions in the structure of magnesium astrophyllite (Shi *et al*. 1998) indicates 13 sites in general positions occupied by divalent anions [O(1) to O(13)], and two sites in general positions occupied by monovalent anions [O(14) and O(15)]. As F does not play a significant role in magnesium astrophyllite (0.07 *apfu* F; Shi *et al*. 1998), the two monovalent anions are assumed to be OH^-. The main difference between the

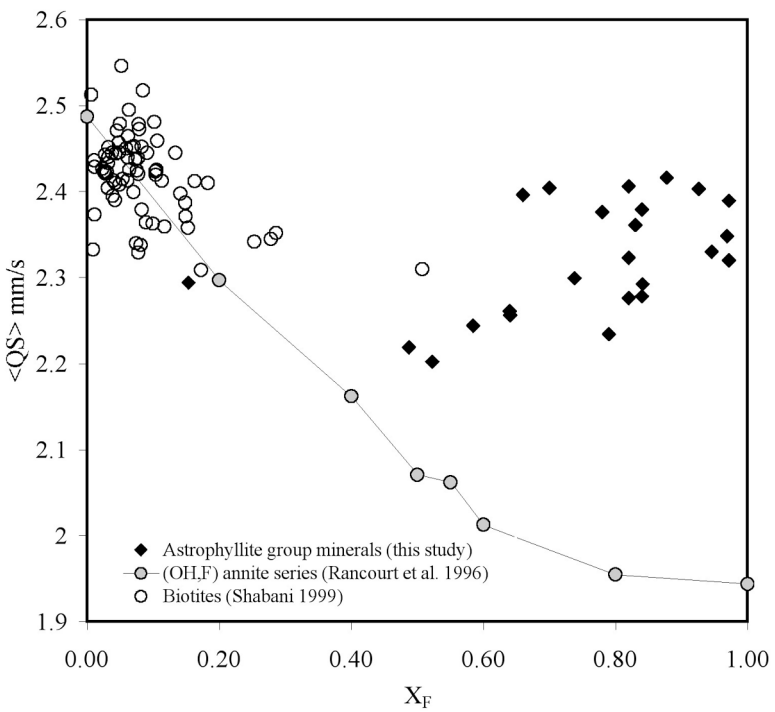

FIG. 4. Average quadrupole splitting, <QS>, *versus* the fraction of F (X_F) for members of the astrophyllite-group and micas of the biotite series.

structure of magnesium astrophyllite and that of other members of the group is the presence of a TiO_5 tetragonal pyramid, unlike the $D\phi_6$ octahedra present in other species. The presence of such a coordination polyhedron results in the absence of one anion [*i.e.*, a vacancy at $\phi(16)$] in the formula for magnesium astrophyllite relative to that of other members of the group. As such, the corresponding anionic scheme for magnesium astrophyllite should be written $O_{26}(OH)_4\square$, rather than $O_{24}(OH)_4(OH,F)_2$ [as reported by Shi *et al.* (1998)].

Given this situation, calculated H_2O contents should approach 3.00 wt.%, with an additional maximum F content of 1.00 wt.%. Direct determinations of volatile components by thermal decomposition indicate contents between 3.55 and 4.00 wt.%, attributable mainly to OH^-, although portions of these are known to include adsorbed, absorbed or molecular H_2O weakly bound in the interlayer. Results of thermogravimetric analyses, which indicate $\Sigma(H_2O + F) \approx 4.00$ wt.%, and of NRA (3.9–5.0 *apfu* H) also support the anionic scheme $O_{26}(OH)_4(F,O,OH)$. No evidence exists in support of the currently accepted anionic scheme, $O_{24}(OH,F)_7$, which would correspond to $\Sigma(H_2O + F) \approx 5.00$ wt.%.

Results of the Current Study: Cationic Composition

The detailed crystal chemistry of each component of the structure can be found below under *Site Chemistry*; details given here is a summary of the site populations.

The interlayer

Results from single-crystal X-ray refinements show that *A* and *B* are crystallographically distinct: $^{[10]-[13]}A$ and $^{[10]}B$. Potassium is the dominant cation at *A*, with variable incorporation of Cs, Rb and Sr. There is no evidence for H_3O^+, as was suggested by proponents of hydroastrophyllite (Hubei Geologic College 1974). The *B* site hosts only Na and Ca. Vacancies at *A* are common, with cation totals often as low as 1.71 *apfu* (ideally 2.00 *apfu*). There is no evidence for the presence of vacancies at *B*.

The O sheet (*C*)

The *O* sheet contains four distinct octahedral sites, *M*(1) to *M*(4), in a 2:2:2:1 proportion ($\Sigma C = 7.00$ *apfu*). The largest of the four octahedra, *M*(1), has been found to be occupied by Mn, Fe^{2+} and Na; *M*(2), *M*(3) and *M*(4) are occupied by Mn, Fe^{2+}, Fe^{3+}, Mg and Zn. There is no evidence for $^{[6]}$Al. Mössbauer spectroscopy indicates that all Fe occurs in the *O* sheet, with Fe^{3+}/Fe_{tot} ranging from 0.01 to 0.21, corresponding to 0.05 to 0.56 *apfu* Fe^{3+}.

The H sheet (*D and T*)

The *H* sheet has the ideal composition $[TiSi_4O_{12}]^{4-}$, with extensive Ti ⇔ (Nb,Zr) substitution. It consists of open-branched *zweier* [100] single chains of $[Si_4O_{12}]^{8-}$ (Liebau 1985), which are in turn cross-linked by corner-sharing $D\phi_6$ octahedra in triclinic species and kupletskite-*Ma2b2c*, and by TiO_5 tetragonal pyramids in magnesium astrophyllite (Shi *et al*. 1998). There are four distinct *T* sites ($\Sigma T = 8.00$ *apfu*) occupied dominantly by Si, with only minor Al-for-Si substitution. Mössbauer spectroscopy has indicated that Fe^{3+} is not present at the *T* sites of the structure. Similarly, neither Fe^{2+} nor Fe^{3+} are found to occur at *D*, which is occupied predominantly by Ti, Zr and Nb, with minor incorporation of Hf and Ta ($\Sigma D = 2.00$ *apfu*).

Proposed General Formula for Astrophyllite-Group Minerals

The general formula proposed for any astrophyllite-group minerals, based on the results described above, is:

$$A_2BC_7D_2T_8O_{26}(OH)_4X_{0-1} \quad (6)$$

where $^{[10]-[13]}A$ = K, Rb, Cs, Na, H_2O and □; $^{[10]}B$ = Na or Ca; $^{[6]}C$ = Mn, Fe^{2+}, Fe^{3+}, Na, Mg, or Zn; $^{[5]-[6]}D$ = Ti, Nb, or Zr; $^{[4]}T$ = Si and Al; and $X = \phi$ = F, OH, O or □. Calculation of general formulae should be based on a total of 31 anions with 26 O and 5(OH,F,O,□). For magnesium astrophyllite, which has a vacant *X* site, the formula should be based on 30 anions with $O_{26}(OH,F)_4$. To account for the variability in *X* resulting from the Ti + F ⇔ Nb + O substitution, two methods of formula calculation are proposed, depending on the Nb_2O_5 content in the sample in question. If Nb_2O_5 is less than 5.00 wt.% (~0.5 *apfu* Nb), the formula should be calculated assuming 26O and 5(OH,F). If Nb_2O_5 is greater than 5.00 wt.%, the formula should be calculated assuming 26O, 4(OH) and one (F,O).

Considering results from single-crystal X-ray structure refinements and EMPA data, we recommend that cations in the general formula be assigned to structural sites according to the following scheme:

i) Sum *T* to 8.00 using Si, then Al;

ii) Sum *D* to 2.00 using Ti, Nb, Zr, Ta and Hf;

iii) Sum *C* to 7.00 using Mn and Fe^{2+}, followed by Fe^{3+}, Mg, Zn, Ce, Y and Na;

iv) Sum *B* to 1.00 first with Ca, then with Na;

v) Sum *A* to 2.00 using excess Na from *C* and *B*, then K, Rb, Cs, Sr and Ba.

Type specimens of zircophyllite, cesium kupletskite and hydroastrophyllite could not be obtained for analysis and confirmation of their anionic scheme. Such species still have their formulae defined by 7(OH,F) in the literature. Table 2 lists the original and revised general formulae for AGM.

Site Chemistry

Table 3 lists representative results of EMPA and calculated formulae, based on the general formula proposed above, for 31 representative samples of astrophyllite-group minerals. Samples have been subdivided on the basis of their geological environment into two categories: those from SiO_2-undersaturated intrusions and those from SiO_2-oversaturated intrusions (OVER). Owing to the wide range of chemical compositions that is observed in the undersaturated category, samples have been further divided into two separate populations on the basis of their Mn# [*i.e.*, Mn/(Mn + Fe_{tot})]: (1) Fe-dominant (FEU) or the *astrophyllite subgroup*, and (2) Mn-dominant (MNU) or the *kupletskite subgroup*. Figure 5 shows the range in compositions observed in this study. Table 4 lists the mean and range of compositions observed in the sample suite.

The interlayer sites (A and B)

All minerals studied are K-dominant at the *A* site(s). Potassium contents range from 1.35 to 2.07 *apfu*, with samples of the astrophyllite subgroup from undersaturated suites having the highest K contents (average: 1.76 *apfu*) and the samples from oversaturated intrusions being the most depleted in K (average: 1.59 *apfu*). Other cations substituting for K at *A* include Rb, Cs, Sr, Ba and Na. Figure 6 shows the range of compositions observed in the interlayer for FEU, MNU and OVER samples. The presence of vacancies at *A* has been confirmed through single-crystal X-ray structure refinement, resulting in cation sums at *A* as low as 1.71 *apfu* (*i.e.*, 15% vacancies).

Rubidium occurs in concentrations up to 0.20 *apfu*, with samples from oversaturated intrusions displaying the highest average contents (0.11 *apfu*), whereas samples from undersaturated intrusions display slightly lower contents (0.06 and 0.08 *apfu*, respectively). As shown by Ganzeyev *et al.* (1969), the extent of the Cs-for-K substitution is more limited than that of Rb-for-K. The highest Cs contents occur in samples from undersaturated intrusions, with a maximum of 0.16 (astrophyllite subgroup) and 0.11 *apfu* (kupletskite subgroup). Cesium enrichments approaching those observed in astrophyllite from Dara-i-Pioz (10.08 wt.% Cs_2O, Ganzeyev *et al.* 1969) or in cesium kupletskite (Efimov *et al.* 1971) were not observed in any of the samples studied.

Ganzeyev *et al.* (1969) proposed that K and Na occur in crystallographically distinct sites and do not substitute isomorphously in the structure. This proposal is confirmed by both single-crystal X-ray structure data (which indicate that two crystallographically distinct interlayer sites, *A* and *B*, host K and Na, respectively), and by EMPA (which indicate that Na ⇔ K substitution is limited, occurring up to a maximum of 24.5% of available *A* sites; 0.49 *apfu* Na in kupletskite from MSH). Lithium occurs in trace concentrations in the samples studied, with contents ranging from 43 to 453 ppm.

TABLE 2. MEMBERS OF THE ASTROPHYLLITE GROUP: ORIGINAL AND REVISED FORMULAE

Species	Original formula	Revised Formula
[1] Niobokupletskite	$K_2Na(Mn,Zn,Fe)_7(Nb,Zr,Ti)_2Si_8O_{26}(OH)_4(O,F)$	unchanged
[2,3] Kupletskite	$(K,Na)_3(Mn,Fe^{2+})_7(Ti,Nb)_2Si_8O_{24}(O,OH)_7$	$K_2Na(Mn,Fe^{2+})_7(Ti,Nb)_2Si_8O_{26}(OH)_4F$
[4] Cesium kupletskite	$(Cs,K,Na)_3(Mn,Fe,Li)_7(Ti,Nb)_2Si_8O_{24}(O,OH,F)_7$	$(Cs,K)_2Na(Mn,Fe,Li)_7(Ti,Nb)_2Si_8O_{26}(OH)_4F$
[5] Astrophyllite	$(K,Na)_3(Fe^{2+},Mn)_7Ti_2Si_8O_{24}(O,OH)_7$	$K_2Na(Fe^{2+},Mn)_7Ti_2Si_8O_{26}(OH)_4F$
[6] Magnesium astrophyllite	$K_2NaNa(Fe,Mn)_4Mg_2Ti_2(Si_4O_{12})_2(OH)_4(OH,F)_2$	$K_2Na[Na(Fe, Mn)_4Mg_2]Ti_2Si_8O_{26}(OH)_4\square$
[7] Niobophyllite	$(K,Na)_3(Fe^{2+},Mn)_6(Nb,Ti)_2Si_8O_{24}(O,OH,F)_7$	$K_2Na(Fe^{2+},Mn)_7(Nb,Ti)_2Si_8O_{26}(OH)_4(F,O)$
[8] Zircophyllite	$(K,Na,Ca,Mn)_3(Fe^{2+},Mn)_7(Zr,Nb)_2Si_8O_{27}(OH,F)_4$	$K_2(Na,Ca)(Mn,Fe^{2+})_7(Zr,Nb)_2Si_8O_{26}(OH)_4F$
* Fe-dominant analogue of zircophyllite		$K_2(Na,Ca)(Fe^{2+},Mn)_7(Zr,Nb)_2Si_8O_{26}(OH)_4F$
[9] Hydroastrophyllite	$(H_3O,K,Ca)_3(Fe^{2+},Mn)_{5-6}Ti_2Si_8(O,OH)_{31}$	$(H_3O,K)_2Ca(Fe^{2+},Mn)_{5-6}Ti_2Si_8O_{26}(OH)_4F$

[1] Piilonen *et al.* (2000), [2] Semenov (1956), [3] Piilonen *et al.* (2001), [4] Efimov *et al.* (1971), [5] Woodrow (1967), [6] Shi *et al.* (1998), [7] Nickel *et al.* (1964), [8] Kapustin (1973), [9] Hubei Geologic College (1974). * A potentially new species, not yet IMA-approved.

However, Li contents up to 0.59 wt.% Li_2O have been noted in astrophyllite from Dara-i-Pioz, Russia (Ganzeyev *et al.* 1969).

Ten-coordinated Na (*B*) is located in the interlayer in a cage between bridging ϕ(16) anions. The average Na content for all samples in this study is 0.83 *apfu*, and Na is the dominant cation at *B* in all cases. The only other cation observed to substitute for Na is Ca, up to a maximum occupancy of 48%. The Ca content in samples from undersaturated intrusions ranges from zero to 0.48 *apfu*, with an average of 0.14 *apfu* in members of the kupletskite subgroup and 0.28 *apfu* in members of the astrophyllite subgroup. Samples from oversaturated intrusions show a range in Ca content from 0.01 to 0.40 *apfu*, the average being 0.08 *apfu*. The Ca content of all samples correlates negatively with Na content, the two being related by the coupled substitution Ca + Al ⇔ Si + Na.

Figure 7 shows the correlation between (K + Na_{tot}), the dominant interlayer cations, and the substituting cations (Rb + Cs + Sr + Ba + Ca). All points plotting above the 1:1 line represent cases in which the sum of cations at *A* and *B* exceeds the ideal value of 3.00 *apfu*. This discrepancy is generally due to an excess of Na, which must be subsequently allocated to the [6]-coordinated *C* sites, a feature discussed in the following section.

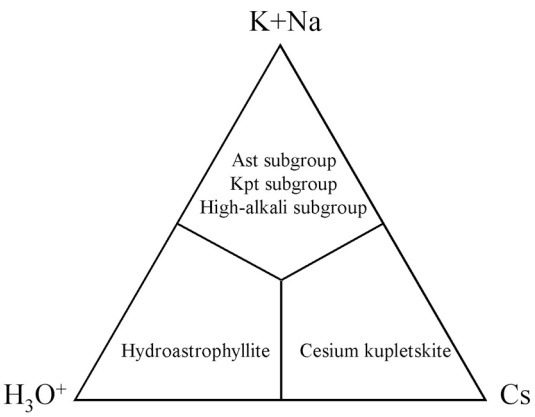

FIG. 5a. Diagram depicting members of the astrophyllite group on the basis of the predominant cation at *A*. All samples in this study represent K-dominant species. Ast: astrophyllite, Kpt: kupletskite.

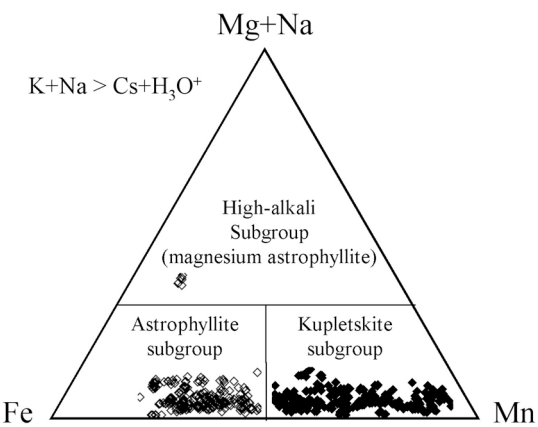

FIG. 5b. Diagram depicting members of the astrophyllite group on the basis of the predominant cation at *C*.

The O sheet: C and Fe^{2+}/Fe^{3+} values

The substitution of Mn for Fe^{2+} at *C* results in a complete solid-solution series (96% observed) between astrophyllite and kupletskite (Fig. 8). This is the dominant mechanism of substitution observed in all

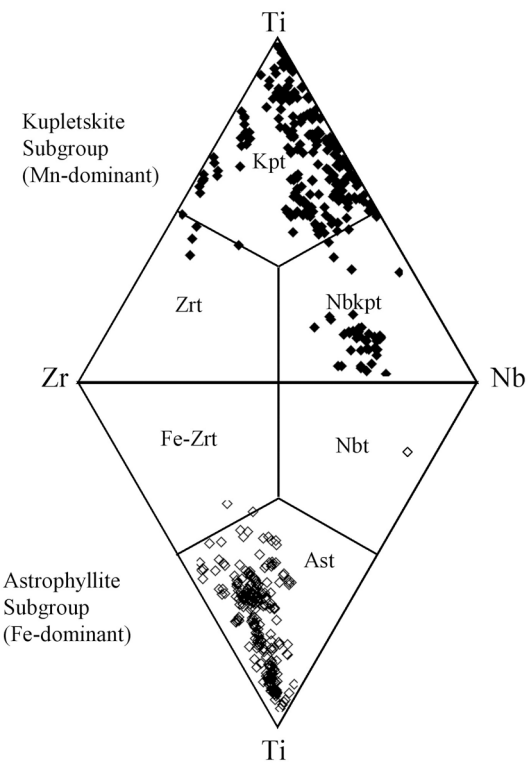

FIG. 5c. Diagram depicting members of the astrophyllite group on the basis of the predominant cation at *D*. Kpt: kupletskite, Zrt: zircophyllite, Nbkpt: niobokupletskite, Fe–Zrt: Fe-dominant analogue of zircophyllite, Nbt: niobophyllite, Ast: astrophyllite.

TABLE 3. REPRESENTATIVE COMPOSITIONS OF ASTROPHYLLITE-GROUP MINERALS*

Loc.	SD	MSH	MSH	MSH	MSH	MSH	MSH	MSH	MSH	MSH	MSH	MSH	MSH	MSH	LANG	LANG	GJER
Sam-	(ave.)	MSH	MSH	MSH	10A	10B	18A	18B	29	31	38B	42	44	45	NOR	NOR	NOR
ple #	%	2	3	7											1	2	3
*n***		13	10	7	5	6	6	2	5	4		3	4	6	11	12	10
Na_2O	1.7	3.51	3.87	2.09	2.44	2.38	2.40	2.21	2.24	1.74	2.45	2.62	1.99	2.64	2.54	1.99	3.52
K_2O	1.0	5.11	5.37	5.76	6.13	6.11	5.97	5.47	5.93	6.24	5.97	5.97	6.19	5.78	5.48	6.19	5.69
Rb_2O	2.5	0.35	0.81	0.40	0.47	0.67	0.49	0.78	0.42	0.38	0.46	0.82	0.33	0.57	0.75	0.36	0.37
Cs_2O	35.0	0.00	0.03	0.01	0.00	0.00	0.02	0.04	0.07	0.02	0.00	0.12	0.09	0.03	1.01	0.21	0.03
CaO	2.0	0.40	0.00	1.13	0.26	0.00	0.54	0.43	1.42	1.18	0.67	0.00	0.37	0.56	1.08	1.31	0.41
SrO	25.0	0.15	0.06	0.24	0.06	0.00	0.11	0.16	0.21	0.24	0.22	0.00	0.04	0.01	0.07	0.08	0.07
BaO	25.0	0.11	0.00	0.00	0.00	0.00	0.00	0.00	0.27	0.00	0.00	n.a.	0.00	0.00	0.00	0.00	0.00
MgO	3.0	0.46	0.51	1.21	0.53	0.16	0.41	0.44	1.49	0.59	0.12	0.15	0.18	0.68	0.81	0.76	0.36
MnO	1.5	32.38	28.11	19.34	19.95	26.98	20.06	15.51	8.50	9.83	23.62	26.37	7.12	22.70	12.48	9.15	17.63
FeO	1.0	2.00	0.71	15.15	13.94	7.05	15.09	20.49	25.45	26.02	10.83	2.64	28.94	10.65	21.23	25.90	16.01
ZnO	21.0	0.75	5.15	0.03	0.43	0.03	0.20	0.00	0.04	0.00	0.26	4.08	0.00	0.43	0.39	0.12	0.47
Al_2O_3	1.6	0.33	0.24	1.23	1.12	1.28	1.05	0.98	1.04	1.40	0.56	1.14	1.35	0.78	0.71	1.27	0.10
Y_2O_3	99.0	0.00	0.00	0.00	0.00	0.00	0.00	0.00	0.00	0.00	0.00	n.a.	0.00	0.00	0.00	0.00	0.00
Ce_2O_3	30.0	0.13	0.00	0.15	0.00	0.00	0.03	0.00	0.17	0.13	0.00	n.a.	0.30	0.00	0.11	0.11	0.23
TiO_2	0.8	11.07	6.64	6.93	5.48	0.73	6.93	6.72	10.57	7.24	6.23	1.34	5.87	7.43	9.71	7.79	9.74
SnO_2	99.0	0.00	0.00	0.00	0.00	0.00	0.00	0.00	0.00	0.00	0.00	n.a.	0.00	0.00	0.05	0.21	0.00
ZrO_2	2.0	0.02	0.07	5.80	1.87	4.18	0.93	4.37	1.42	4.25	9.11	3.43	4.47	0.34	1.85	4.50	1.07
HfO_2	99.0	0.02	0.00	0.22	0.00	0.00	0.00	0.13	0.00	0.13	0.00	0.00	0.00	0.00	0.01	0.11	0.00
Nb_2O_5	2.0	1.72	8.02	1.26	8.06	12.34	6.92	2.53	1.39	2.47	0.71	12.13	4.50	6.90	1.73	1.74	2.27
Ta_2O_5	31.0	0.07	0.00	0.06	0.23	0.56	0.00	0.00	0.00	0.14	0.00	0.63	0.03	0.08	0.00	0.13	0.09
SiO_2	0.5	34.66	33.66	32.00	33.14	31.75	32.82	32.66	33.77	31.89	33.53	31.85	32.81	34.35	34.96	33.87	34.92
F	10.0	1.21	0.80	1.28	0.67	0.20	0.88	1.21	1.37	1.18	1.34	0.14	0.94	0.89	1.15	1.04	1.65
H_2O	n.b.	2.75	2.58	2.60	2.59	2.50	2.59	2.63	2.69	2.67	2.62	2.48	2.80	2.69	2.80	2.83	2.52
O=F	n.b.	-0.51	-0.34	-0.54	-0.28	-0.09	-0.37	-0.51	-0.57	-0.50	-0.56	-0.06	-0.40	-0.38	-0.48	-0.44	-0.69
Total	n.b.	96.71	96.34	96.35	97.06	96.82	97.03	96.21	97.90	97.20	98.13	95.85	97.89	97.10	98.43	99.24	96.44
							formulae based on 31 anions										
Na	1.7	0.49	0.49	0.23	0.04	0.06	0.21	0.11	0.23	0.08	0.04	0.00	0.00	0.00	0.06	0.09	0.31
K	1.0	1.47	1.59	1.72	1.81	1.87	1.76	1.64	1.70	1.85	1.75	1.84	1.82	1.68	1.57	1.78	1.65
Rb	2.5	0.05	0.12	0.06	0.07	0.10	0.07	0.12	0.06	0.06	0.07	0.13	0.05	0.08	0.11	0.05	0.05
Cs	35.0	0.00	0.00	0.00	0.00	0.00	0.00	0.00	0.01	0.00	0.00	0.01	0.01	0.00	0.10	0.02	0.00
Sr	25.0	0.02	0.01	0.03	0.01	0.00	0.02	0.02	0.03	0.03	0.03	0.00	0.01	0.00	0.01	0.01	0.01
Ba	25.0	0.01	0.00	0.00	0.00	0.00	0.00	0.00	0.02	0.00	0.00	0.00	0.00	0.00	0.00	0.00	0.00
Sum *A*	n.b.	2.04	2.22	2.04	1.93	2.03	2.06	1.89	2.05	2.02	1.89	1.98	1.89	1.77	1.84	1.95	2.03
Na	1.7	0.90	1.00	0.72	0.94	1.00	0.87	0.89	0.66	0.71	0.84	0.95	0.89	0.86	0.74	0.68	0.90
Ca	2.0	0.10	0.00	0.28	0.06	0.00	0.13	0.11	0.34	0.29	0.17	0.00	0.09	0.14	0.26	0.32	0.10
Sum *B*	n.b.	1.00	1.00	1.00	1.00	1.00	1.00	1.00	1.00	1.00	1.00	0.95	0.98	1.00	1.00	1.00	1.00
Na	1.7	0.14	0.26	0.00	0.12	0.05	0.00	0.00	0.09	0.00	0.22	0.28	0.00	0.30	0.30	0.09	0.34
Mg	3.0	0.16	0.18	0.42	0.18	0.06	0.14	0.15	0.50	0.20	0.04	0.05	0.06	0.23	0.27	0.25	0.12
Mn	1.5	6.19	5.54	3.83	3.92	5.48	3.93	3.08	1.62	1.94	4.61	5.40	1.39	4.38	2.37	1.75	3.40
Fe^{2+}	1.0	0.38	0.14	2.96	2.70	1.41	2.92	4.01	4.78	5.07	2.09	0.53	5.59	2.02	3.98	4.88	3.05
Zn	21.0	0.12	0.89	0.00	0.07	0.01	0.03	0.00	0.01	0.00	0.04	0.73	0.00	0.07	0.06	0.02	0.08
Y	99.0	0.00	0.00	0.00	0.00	0.00	0.00	0.00	0.00	0.00	0.00	0.00	0.00	0.00	0.00	0.00	0.00
Ce	30.0	0.01	0.00	0.01	0.00	0.00	0.00	0.00	0.01	0.01	0.00	0.00	0.03	0.00	0.01	0.01	0.02
Sum *C*	n.b.	7.00	7.00	7.23	7.00	7.00	7.03	7.24	7.00	7.22	7.00	7.00	7.07	7.00	6.70	6.91	6.66
Ti	0.8	1.88	1.16	1.21	0.95	0.13	1.21	1.18	1.79	1.27	1.08	0.24	1.02	1.27	1.64	1.32	1.67
Sn	99.0	0.00	0.00	0.00	0.00	0.00	0.00	0.00	0.00	0.00	0.00	0.00	0.00	0.00	0.00	0.02	0.00
Zr	2.0	0.00	0.01	0.66	0.21	0.49	0.10	0.50	0.16	0.48	1.02	0.41	0.50	0.04	0.20	0.49	0.12
Hf	99.0	0.00	0.00	0.01	0.00	0.00	0.00	0.01	0.00	0.01	0.00	0.00	0.00	0.00	0.00	0.01	0.00
Nb	2.0	0.18	0.84	0.13	0.85	1.34	0.72	0.27	0.14	0.26	0.07	1.33	0.47	0.71	0.18	0.18	0.23
Ta	31.0	0.00	0.00	0.00	0.01	0.04	0.00	0.00	0.00	0.01	0.00	0.04	0.00	0.01	0.00	0.01	0.01
Sum *D*	n.b.	2.06	2.01	2.03	2.03	1.99	2.03	1.96	2.08	2.03	2.18	2.02	1.99	2.02	2.02	2.02	2.02
Si	0.5	7.82	7.83	7.48	7.69	7.61	7.59	7.65	7.58	7.42	7.72	7.71	7.58	7.81	7.84	7.63	7.94
Al	1.6	0.09	0.07	0.34	0.31	0.36	0.29	0.27	0.28	0.38	0.15	0.33	0.37	0.21	0.19	0.34	0.03
Sum *T*	n.b.	7.91	7.90	7.82	7.99	7.97	7.88	7.92	7.86	7.80	7.88	8.03	7.95	8.02	8.03	7.96	7.97
F	10.0	0.86	0.59	0.95	0.49	0.15	0.64	0.89	0.97	0.87	0.98	26.89	0.69	0.64	0.82	0.74	1.18
OH	n.b.	4.14	4.00	4.05	4.00	4.00	4.00	4.11	4.03	4.13	4.02	4.00	4.31	4.07	4.18	4.26	3.82
O	n.b.	30.14	30.41	30.05	30.51	30.85	30.36	30.11	30.03	30.13	30.02	30.11	30.31	30.36	30.18	30.26	29.82
Σ cat.	n.b.	20.01	20.14	20.11	19.95	19.99	20.00	20.01	19.99	20.07	19.95	19.98	19.88	19.81	19.89	19.94	20.02
Mn#	n.b.	0.94	0.98	0.56	0.59	0.80	0.57	0.43	0.25	0.28	0.68	0.91	0.20	0.68	0.37	0.26	0.53

* Electron-microprobe data, ** Number of analyses made, n.a.: not analyzed for, n.b.: not determined, SD: Standard deviation, Mn# = $Mn/(Mn + Fe_{tot})$. The compositions are quoted in weight %, then in atoms per formula unit (*apfu*).

TABLE 3. REPRESENTATIVE COMPOSITIONS OF ASTROPHYLLITE-GROUP MINERALS (continued)*

Loc.	SD	LANG	LANG	LUKS	KHIB	KHIB	KHIB	LOV	PP	POR	AFR	LAB	EGY	EGY	GRE	GRE	GRE
Sam-	(ave.)	NOR	NOR	NOR	RUS	RUS	RUS	RUS	US	US	AFR	LAB	R	R	CC	CC	CC
ple #	%	10	14	21	1	3	6	9	1	9	1	2	1200	3090	4	7A	7B
*n***		4	4	8	7	7	7	4	8	7	6	3	1	1			
Na_2O	1.7	1.88	2.64	2.88	2.21	2.54	4.68	2.09	2.66	2.80	2.53	2.67	2.73	3.14	2.78	2.49	3.15
K_2O	1.0	5.75	5.93	5.46	6.25	5.95	7.58	6.08	5.07	5.21	5.49	5.84	6.23	5.72	5.62	6.07	5.66
Rb_2O	2.5	0.67	0.35	0.47	0.26	0.24	0.17	0.40	1.28	1.06	0.46	0.49	n.a.	n.a.	n.a.	n.a.	n.a.
Cs_2O	35.0	0.28	0.01	0.12	0.01	0.03	0.00	0.00	0.14	0.09	0.10	0.31	n.a.	n.a.	n.a.	n.a.	n.a.
CaO	2.0	1.05	0.85	0.46	1.77	1.66	0.94	1.08	0.21	0.82	0.52	0.31	0.35	0.24	0.65	1.18	0.56
SrO	25.0	0.09	0.04	0.04	0.30	0.27	0.07	0.20	0.00	0.03	0.07	0.00	n.a.	n.a.	n.a.	n.a.	n.a.
BaO	25.0	0.00	0.00	0.02	0.16	0.18	0.17	0.43	0.11	0.00	0.15	0.00	n.a.	n.a.	n.a.	n.a.	n.a.
MgO	3.0	0.85	1.95	0.38	1.38	1.40	6.27	1.23	0.04	0.21	0.00	0.00	0.02	0.02	0.68	0.96	1.15
MnO	1.5	13.12	18.98	9.55	5.69	5.39	2.19	21.47	3.44	23.25	5.17	8.76	1.37	1.55	7.62	11.60	12.68
FeO	1.0	21.43	13.29	24.50	28.25	28.37	20.66	12.18	30.06	11.00	30.03	24.20	34.54	34.42	28.76	23.43	21.82
ZnO	21.0	0.26	0.51	0.68	0.00	0.00	0.00	0.00	1.85	0.00	0.50	0.06	0.39	0.89	n.a.	n.a.	n.a.
Al_2O_3	1.6	1.28	0.63	0.23	1.29	1.07	0.37	0.92	0.22	0.67	0.44	1.16	0.69	0.43	0.40	1.12	0.56
Y_2O_3	99.0	0.00	0.00	0.00	0.00	0.00	0.00	0.00	0.00	0.00	0.00	0.00	n.a.	n.a.	n.a.	n.a.	n.a.
Ce_2O_3	30.0	0.28	0.00	0.00	0.09	0.05	0.02	0.22	0.06	0.00	0.06	0.07	n.a.	n.a.	n.a.	n.a.	n.a.
TiO_2	0.8	7.96	10.02	10.02	11.22	11.40	12.78	9.74	9.09	8.97	7.48	3.23	9.74	9.23	10.63	10.24	10.84
SnO_2	99.0	0.09	0.00	0.00	0.00	0.00	0.00	0.00	0.75	0.00	1.80	0.00	0.16	0.44	n.a.	n.a.	n.a.
ZrO_2	2.0	3.93	0.85	1.13	0.82	0.68	0.00	0.47	0.80	0.49	2.59	0.00	2.24	1.61	0.69	1.69	1.02
HfO_2	99.0	0.11	0.00	0.01	0.00	0.00	0.00	0.00	0.04	0.00	0.18	0.00	n.a.	n.a.	n.a.	n.a.	n.a.
Nb_2O_5	2.0	1.99	2.74	1.66	0.79	0.74	1.18	2.94	3.21	3.56	2.03	14.15	1.50	2.01	1.38	1.17	1.42
Ta_2O_5	31.0	0.00	0.12	0.00	0.16	0.16	0.15	0.00	0.00	0.00	1.18	0.10	n.a.	n.a.	n.a.	n.a.	n.a.
SiO_2	0.5	33.41	35.29	35.42	34.27	34.95	38.64	34.72	34.83	34.90	33.98	34.00	35.74	35.50	35.70	34.90	35.94
F	10.0	1.13	1.00	1.43	1.13	1.22	0.11	1.02	1.12	1.08	1.05	0.14	1.46	1.77	0.94	0.93	0.88
H_2O	n.b.	2.75	2.91	2.63	2.84	2.82	3.57	2.87	2.75	2.79	2.76	2.60	2.69	2.52	2.94	2.94	3.00
O=F	n.b.	-0.48	-0.42	-0.60	-0.48	-0.51	-0.05	-0.43	-0.47	-0.45	-0.44	-0.06	n.a.	n.a.	0.40	0.39	0.37
Total	n.b.	97.81	97.67	96.48	98.41	98.60	99.50	97.62	97.63	96.47	98.09	98.03	99.85	99.49	98.39	98.32	98.30
formulae based on 31 anions																	
Na	1.7	0.07	0.09	0.08	0.15	0.18	0.00	0.00	0.00	0.07	0.13	0.00	0.00	0.13	0.31	0.19	0.22
K	1.0	1.68	1.68	1.58	1.77	1.67	2.00	1.74	1.48	1.51	1.61	1.72	1.73	1.60	1.59	1.72	1.59
Rb	2.5	0.10	0.05	0.07	0.04	0.03	0.02	0.06	0.19	0.16	0.07	0.07	n.a.	n.a.	n.a.	n.a.	n.a.
Cs	35.0	0.03	0.00	0.01	0.00	0.00	0.00	0.00	0.01	0.01	0.01	0.03	n.a.	n.a.	n.a.	n.a.	n.a.
Sr	25.0	0.01	0.00	0.00	0.04	0.03	0.01	0.03	0.00	0.00	0.01	0.00	n.a.	n.a.	n.a.	n.a.	n.a.
Ba	25.0	0.00	0.00	0.00	0.01	0.02	0.01	0.04	0.01	0.00	0.01	0.00	n.a.	n.a.	n.a.	n.a.	n.a.
Sum *A*	n.b.	1.89	1.82	1.75	2.01	1.94	2.05	1.86	1.69	1.75	1.84	1.82	1.73	1.73	1.90	1.91	1.81
Na	1.7	0.74	0.80	0.89	0.58	0.61	0.78	0.69	0.95	0.78	0.87	0.92	0.92	0.94	0.85	0.72	0.87
Ca	2.0	0.26	0.20	0.11	0.42	0.39	0.21	0.26	0.05	0.20	0.13	0.08	0.08	0.06	0.15	0.28	0.13
Sum *B*	n.b.	1.00	1.00	1.00	1.00	1.00	0.99	0.95	1.00	0.98	1.00	1.00	1.00	1.00	1.00	1.00	1.00
Na	1.7	0.02	0.25	0.29	0.22	0.30	1.10	0.22	0.27	0.37	0.13	0.60	0.38	0.26	0.03	0.16	0.25
Mg	3.0	0.29	0.65	0.13	0.46	0.46	1.93	0.41	0.01	0.07	0.00	0.00	0.01	0.01	0.22	0.32	0.38
Mn	1.5	2.54	3.56	1.83	1.07	1.01	0.38	4.07	0.67	4.47	1.01	1.71	0.25	0.29	1.43	2.18	2.36
Fe^{2+}	1.0	4.09	2.46	4.64	5.24	5.23	3.58	2.28	5.74	2.09	5.78	4.67	6.30	6.30	5.32	4.34	4.01
Zn	21.0	0.04	0.08	0.11	0.00	0.00	0.00	0.00	0.31	0.00	0.09	0.01	0.07	0.14	n.a.	n.a.	n.a.
Y	99.0	0.00	0.00	0.00	0.00	0.00	0.00	0.00	0.00	0.00	0.00	0.00	n.a.	n.a.	n.a.	n.a.	n.a.
Ce	30.0	0.02	0.00	0.00	0.01	0.00	0.00	0.02	0.01	0.00	0.00	0.01	n.a.	n.a.	n.a.	n.a.	n.a.
Sum *C*	n.b.	6.98	6.75	7.00	7.00	7.00	7.00	7.00	7.00	7.00	7.01	6.40	7.00	7.00	7.00	7.00	7.00
Ti	0.8	1.37	1.67	1.71	1.87	1.89	1.99	1.64	1.56	1.53	1.29	0.56	1.60	1.52	1.77	1.71	1.79
Sn	99.0	0.01	0.00	0.00	0.00	0.00	0.00	0.00	0.07	0.00	0.17	0.00	0.01	0.04	n.a.	n.a.	n.a.
Zr	2.0	0.44	0.09	0.12	0.09	0.07	0.00	0.05	0.09	0.05	0.29	0.00	0.24	0.17	0.07	0.18	0.11
Hf	99.0	0.01	0.00	0.00	0.00	0.00	0.00	0.00	0.00	0.00	0.01	0.00	n.a.	n.a.	n.a.	n.a.	n.a.
Nb	2.0	0.21	0.27	0.17	0.08	0.07	0.11	0.30	0.33	0.37	0.21	1.48	0.15	0.20	0.14	0.12	0.14
Ta	31.0	0.00	0.01	0.00	0.01	0.01	0.01	0.00	0.00	0.00	0.07	0.01	n.a.	n.a.	n.a.	n.a.	n.a.
Sum *D*	n.b.	2.02	2.04	2.00	2.05	2.05	2.11	1.99	2.05	1.95	2.05	2.04	1.99	1.93	1.98	2.01	2.04
Si	0.5	7.63	7.82	8.02	7.61	7.70	8.00	7.77	7.95	7.93	7.82	7.83	7.79	7.78	7.90	7.74	7.90
Al	1.6	0.34	0.16	0.06	0.34	0.28	0.09	0.24	0.06	0.18	0.12	0.31	0.18	0.11	0.10	0.29	0.15
Sum *T*	n.b.	7.97	7.98	8.08	7.95	7.98	8.09	8.02	8.01	8.11	7.94	8.15	7.97	7.89	8.00	8.03	8.05
F	10.0	0.81	0.70	1.03	0.80	0.85	0.07	0.72	0.81	0.77	0.77	0.10	1.09	1.23	0.66	0.66	0.61
OH	n.b.	4.19	4.30	3.97	4.20	4.15	4.93	4.28	4.19	4.23	4.23	4.00	3.90	3.67	4.34	4.34	4.39
O	n.b.	30.19	30.30	29.97	30.20	30.15	30.93	30.28	30.19	30.23	30.23	30.90	26.00	26.00	26.00	26.00	26.00
Σ cat.	n.b.	19.88	19.85	19.83	20.01	19.97	20.24	19.81	19.73	19.80	19.83	19.67	19.69	19.54	19.88	19.95	19.90
Mn#	n.b.	0.38	0.59	0.28	0.17	0.16	0.10	0.64	0.10	0.68	0.15	0.27	0.04	0.04	0.21	0.33	0.37

* Electron-microprobe data, ** Number of analyses made, n.a.: not analyzed for, n.b.: not determined, SD: Standard deviation, Mn# = $Mn/(Mn + Fe_{tot})$. The compositions are quoted in weight %, then in atoms per formula unit (*apfu*).

astrophyllite-group minerals, regardless of the bulk composition of the *O* sheet or petrogenetic affinity. As noted by other authors (Macdonald & Saunders 1973, Layne *et al.* 1982), minerals of this group from undersaturated intrusions show the strongest enrichment in Mn (up to 6.34 *apfu*; Fig. 9). However, they also show the strongest enrichments in Fe^{2+} (up to 6.71 *apfu*), leading to an extensive range of possible compositions in undersaturated environments alone ($0.09 \leq Mn\# \leq 1.00$). Astrophyllite-group minerals from oversaturated environments show a variable but restricted range of Mn# (0.03 to 0.69) and tend toward Fe-enrichment; only samples from the Gjerdingen ($0.38 \leq Mn\# \leq 0.51$) and Point of Rocks ($0.65 \leq Mn\# \leq 0.69$) intrusions show slight enrichment in the kupletskite component.

The Fe^{3+}/Fe_{tot} values in the samples studied, as determined by Mössbauer spectroscopy, range from 0.01 to 0.21, corresponding to 0.05 to 0.56 *apfu* Fe^{3+} and accounting for a maximum of 8% of *C* (Table 5). Although Fe^{3+} enrichment is minor relative to Fe^{2+} and Mn, a difference in Fe^{3+}/Fe_{tot} is observed between members of the kupletskite and astrophyllite subgroups. The lowest Fe^{3+}/Fe_{tot} values are observed in near-end-member astrophyllite (average: 0.04, range: 0.01 to 0.08) from both over- and undersaturated rocks, whereas the highest values occur predominantly in members of the kupletskite subgroup (average: 0.10, range: 0.04 to 0.21), in particular in Nb-bearing kupletskite and niobokupletskite. The enrichment of Fe^{3+} in such samples is consistent with the "oxidizing" coupled substitution $Ti + F \Leftrightarrow Nb + O$ proposed for incorporation of Nb into the astrophyllite structure (Piilonen *et al.* 2000). It is well documented in other rock-forming minerals (*e.g.* biotites, amphiboles; Czamanske & Mihálik 1972, Czamanske & Wones 1973) that an increase in oxygen fugacity, $f(O_2)$, in alkaline systems results in a decreased activity of Fe^{2+}, increased activity of Fe^{3+}, and a subsequent enrichment in Mn and Mg, concomitant with a decrease in Ti, Al and F. In particular, the dominant magmatic process controlling the distribution of Mn in silicates is the degree of oxidation (Czamanske & Mihálik 1972). It is therefore not surprising that in the astrophyllite group, we observe the highest Fe^{3+}/Fe_{tot} values in Mn-rich samples, suggesting that crystallization proceeded under oxidizing conditions.

Assuming only typical divalent and trivalent cations (*e.g.*, Mn, Fe^{2+}, Fe^{3+}, Mg, Zn, *etc.*) at *C* generally results in low cation sums ($\Sigma C \approx 6.70$ *apfu*). Conversely, in all analytical results, the total Na content is greater than the ideal sum of 1.00 *apfu* for the *B* site. Single-crystal X-ray refinements of the structure of 20 samples indicate the presence of $^{[6]}Na$ at the large *M*(1) site (Piilonen *et al.* 2003). Such refinements have shown that all Ca should be assigned to *B*, with Na added to a sum of 1.00 *apfu.* All excess Na should be assigned to *C*, up to the ideal sum of 7.00 *apfu*. The presence of $^{[6]}Na$ is most likely the result of the extreme peralkalinity and Na activity of the parental melt. Astrophyllite-group minerals from oversaturated rocks show the highest $^{[6]}Na$ content (average: 0.26 *apfu*), with a range from

TABLE 4. MEAN AND RANGE OF CATIONS IN MINERALS OF THE ASTROPHYLLITE GROUP

	Oversaturated			Undersaturated					
				Kupletskite subgroup			Astrophyllite subgroup		
Cation	Mean	Min.	Max.	Mean	Min.	Max.	Mean	Min.	Max.
Na *apfu*	1.21	0.62	1.59	1.22	0.76	1.86	0.92	0.63	1.91
K	1.59	1.41	1.86	1.69	1.35	1.90	1.76	1.43	2.07
Rb	0.11	0.00	0.20	0.08	0.00	0.20	0.06	0.00	0.18
Cs	0.01	0.00	0.03	0.00	0.00	0.11	0.02	0.00	0.16
Sr	0.00	0.00	0.03	0.01	0.00	0.05	0.03	0.00	0.07
Ba	0.01	0.00	0.03	0.00	0.00	0.05	0.01	0.00	0.04
Ca	0.10	0.01	0.47	0.12	0.00	0.39	0.30	0.08	0.48
Mg	0.06	0.00	0.52	0.24	0.03	0.70	0.35	0.06	2.00
Mn	1.48	0.16	4.60	4.77	3.11	6.50	2.03	0.36	3.44
Fe^{2+}	5.04	1.99	6.71	1.79	0.00	3.37	4.53	3.07	5.67
Zn	0.16	0.00	0.82	0.12	0.00	1.73	0.02	0.00	0.11
Ti	1.52	0.51	1.97	1.19	0.10	2.04	1.50	0.82	2.08
Sn	0.04	0.00	0.24	0.00	0.00	0.04	0.00	0.00	0.03
Zr	0.14	0.00	0.35	0.21	0.00	1.02	0.33	0.00	0.81
Hf	0.00	0.00	0.02	0.00	0.00	0.03	0.01	0.00	0.04
Nb	0.31	0.04	1.68	0.61	0.06	1.51	0.19	0.04	0.49
Ta	0.01	0.00	0.13	0.01	0.00	0.05	0.01	0.00	0.04
Si	7.89	7.44	8.08	7.68	7.36	8.01	7.60	7.12	8.13
Al	0.12	0.00	0.54	0.25	0.02	0.73	0.33	0.04	0.53
F	0.89	0.00	1.32	0.63	0.00	1.07	0.81	0.54	1.17
Mn#	0.23	0.02	0.69	0.73	0.50	1.00	0.31	0.09	0.49

TABLE 5. Fe^{2+}/Fe^{3+} VALUES FOR ASTROPHYLLITE-GROUP MINERALS STUDIED BY ^{57}Fe MÖSSBAUER SPECTROSCOPY

Sample #	Mn#	Fe^{2+}/Fe^{3+}	Fe^{3+}/Fe_{tot}	Fe^{3+}
US2	0.10	11.47 (36)	0.08	0.45
US5	0.15	32.33 (30)	0.03	0.16
NOR1	0.37	12.93 (58)	0.07	0.28
NOR9	0.26	17.80 (35)	0.05	0.26
RUS4	0.37	25.39 (56)	0.04	0.14
RUS5	0.26	15.23 (47)	0.06	0.28
RUS7	0.26	85.96 (88)	0.01	0.05
RUS8	0.31	17.80 (98)	0.05	0.21
CC2A	0.13	38.06 (73)	0.03	0.17
CC7A	0.33	46.17 (56)	0.02	0.09
MSH6	0.53	12.81 (91)	0.07	0.22
MSH7	0.56	23.81 (65)	0.04	0.12
MSH10A	0.59	3.84 (97)	0.21	0.56
MSH10B	0.80	3.85 (65)	0.21	0.29
MSH11	0.61	8.17 (85)	0.11	0.28
MSH15	0.81	15.47 (63)	0.06	0.08
MSH18A	0.57	13.16 (69)	0.07	0.21
MSH26A	0.53	11.20 (11)	0.08	0.26
MSH26B	0.41	17.38 (92)	0.05	0.20
MSH28	0.27	71.46 (66)	0.01	0.05
MSH32	0.33	30.06 (45)	0.03	0.14
MSH33	0.38	16.36 (81)	0.06	0.26
MSH34A	0.27	26.32 (78)	0.04	0.20
MSH35	0.52	17.52 (12)	0.05	0.16

Mn# = $Mn/(Mn + Fe_{tot})$. The amount of Fe^{3+} is expressed in *apfu*.

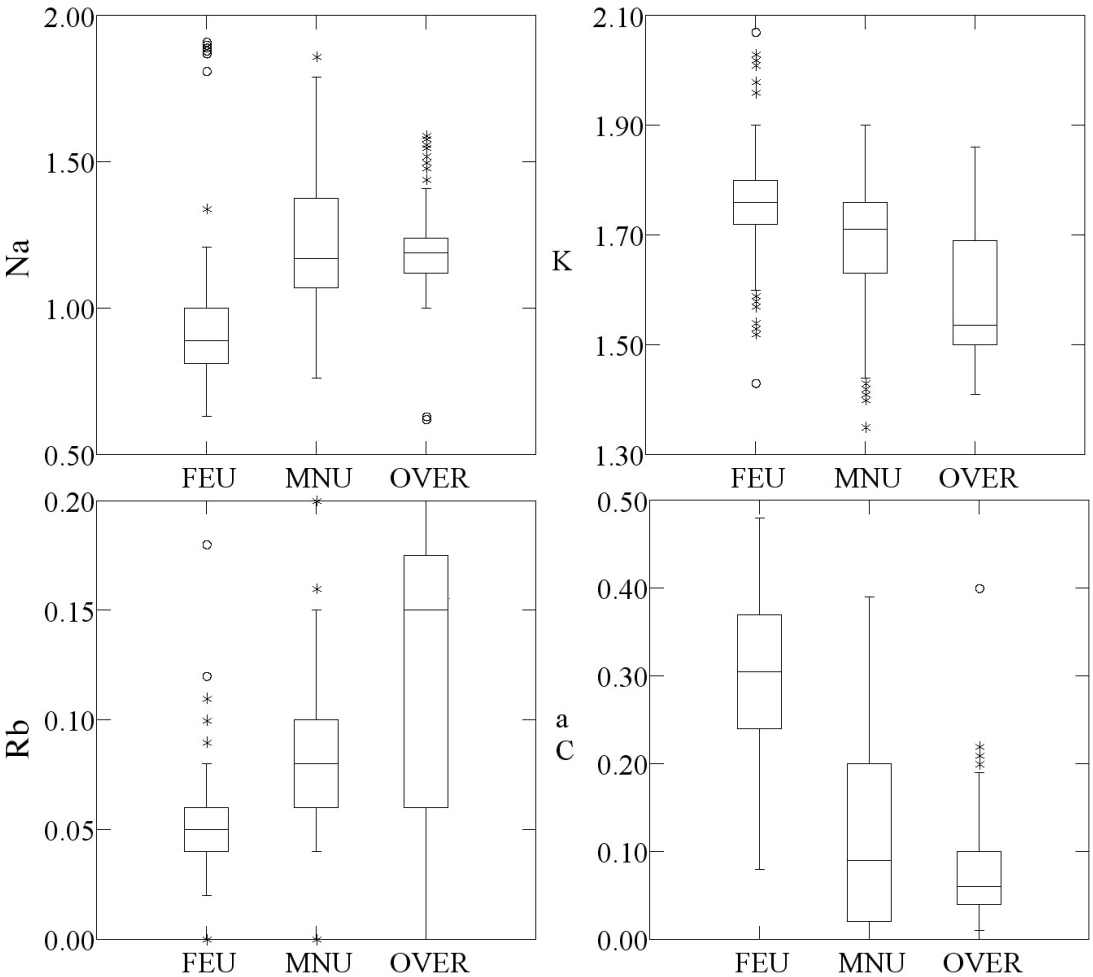

FIG. 6. Boxplots, similar to histograms, are useful tools to graphically depict population distributions and associated statistics (*e.g.*, range, median, mean). Shown here are boxplots depicting the distribution of interlayer cations in astrophyllite-group minerals from silica-undersaturated and silica-oversaturated intrusions. FEU: Fe-dominant, undersaturated; MNU: Mn-dominant, undersaturated; OVER: oversaturated. The central horizontal line of each box represents the median of the sample. The length of each box represents the range within which the central 50% of the values fall (box edges and hinge: 1st and 3rd quartile). Lower and outer fences represent lower and upper hinge ± (1.5•interquartile range). Whiskers represent lower/upper hinge ± (3•interquartile range). Open circles are outliers.

0.07 to 0.43 *apfu*. Kupletskite- and astrophyllite-subgroup samples from undersaturated rocks have slightly lower [6]Na contents (average: 0.11 and 0.09 *apfu*, respectively). In magnesium astrophyllite, Na is the dominant cation at a single [6]-coordinated site within the *O* sheet (average: 1.10 *apfu*), crystallographically equivalent to *M*(1) in triclinic members of the group and kupletskite-*Ma*2*b*2*c*.

Other cations assigned to *C* include Mg and Zn (Fig. 9). Elevated Mg contents occur in samples from undersaturated environments (up to 0.70 *apfu*), with the highest Mg content being observed in magnesium astrophyllite from the Khibina massif, Russia (2.00 *apfu* Mg), a member of the high-alkali subgroup. The presence of a high Mg content appears to require a modification of the structure from triclinic to monoclinic in order to accommodate the smaller Mg cation, with a concomitant occupation of a single *M* site by Na. This modification is not the result of polytypic stacking (*i.e.*, the structure of magnesium astrophyllite cannot be simply related to that of other members of the group by stacking of *HOH* layers; Piilonen *et al.* 2001). Magne-

sium astrophyllite should therefore be considered as a completely different structure-type. As such, the structural differences between magnesium astrophyllite and either astrophyllite- or kupletskite-subgroup members are significant, thus inhibiting extensive solid-solution between them.

Astrophyllite-group minerals from undersaturated environments, in particular members of the kupletskite subgroup, show an extensive range of Zn contents; kupletskite from syenite pegmatites at MSH contain up to 0.91 *apfu* Zn. The presence of high Zn contents supports the observation that astrophyllite-group minerals are concentrators of Zn (Macdonald & Saunders 1973). The positive correlation between Zn and Mn has also been noted in amphiboles from the Strange Lake granite (Quebec; Hawthorne *et al*. 2001) and from the Virgin Canyon pluton (New Mexico; Hawthorne *et al.* 1993, 1994), suggesting a petrogenetic link between elevated Zn contents and oxidizing, Mn-rich alkaline environments. Furthermore, there is evidence that the presence of elevated Zn contents in such environments is not the result of an interaction with host sediments, but that the Zn has a primary magmatic origin; primary Zn minerals such as sphalerite, wurtzite and genthelvite, as well as secondary hemimorphite and hydrozincite, are common in intrusions such as Ilímaussaq (South Greenland) and Mont Saint-Hilaire (Quebec). As was discussed by Piilonen *et al.* (2000), the presence of elevated Zn contents in astrophyllite-group minerals, and possibly in related silicates such as amphiboles, may indicate that the prevailing sulfur fugacity, $f(S_2)$, at the time of crystallization was too low to allow for the crystallization of a distinct Zn–S species (*e.g.* sphalerite, wurtzite).

The H sheet: D site

The *D* site is dominated by high-field-strength elements (Fig. 10). Other elements at *D* include Ta (maximum 0.13 *apfu*) and Hf (maximum 0.04 *apfu*). There is a strong positive correlation between (Zr + Nb) and Ti (Fig. 11), yet correlations between levels of Zr and Nb are poor. This phenomenon has also been noted in eudialyte-group minerals (Johnsen & Gault 1997) and is suggestive of extensive Ti ⇔ Nb and Ti ⇔ Zr substitution, but a lack of Nb ⇔ Zr substitution. Niobium can occupy up to 75% (1.50 *apfu* Nb) of the *D* site in kupletskite-subgroup samples, as observed in niobokupletskite from MSH, and, up to 84% (1.68 *apfu* Nb) of the *D* site in niobophyllite from Letitia Lake (Labrador, Canada). Niobium-bearing kupletskite and niobokupletskite samples from MSH are common hosts of pyrochlore inclusions (up to ~40 μm) in fractures and along cleavages, the result of remobilization of Nb from earlier Nb-bearing silicates by oxidizing, F-rich post-magmatic fluids.

Zirconium shows limited substitution for Ti and Nb (maximum: 1.02 *apfu* in zircophyllite from MSH), an explanation for which may be provided on both crystal-chemical and geochemical grounds. With respect to the

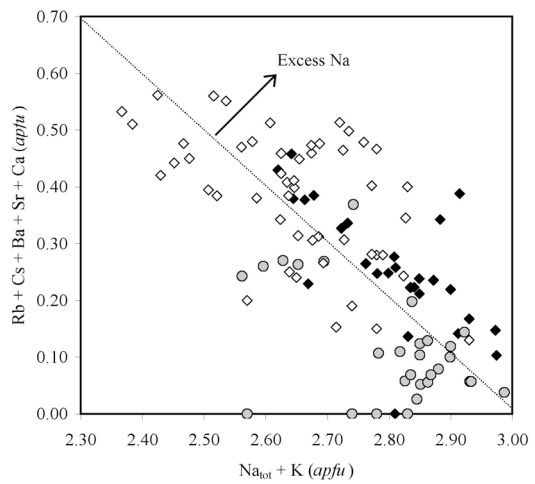

FIG. 7. (K + Na_{tot}) *versus* (Rb + Cs + Sr + Ba + Ca) in the interlayer of astrophyllite-group minerals. The dashed line represents the 1:1 substitution line for an ideal *A* + *B* sum of three *apfu*. Points that plot above the line represent samples with excess Na. Circles: OVER, closed diamonds: MNU, open diamonds: FEU.

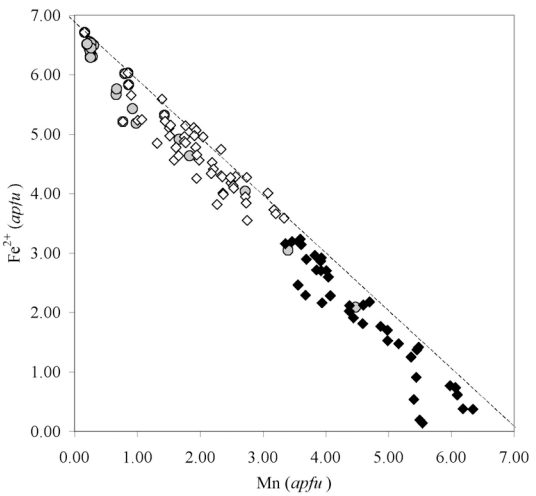

FIG. 8. The content of Mn *versus* that of Fe^{2+} at the *C* site of astrophyllite-group minerals (linear regression, R^2 = 0.977). The 1:1 line is indicated. Circles: OVER, closed diamonds, MNU, open diamonds: FEU.

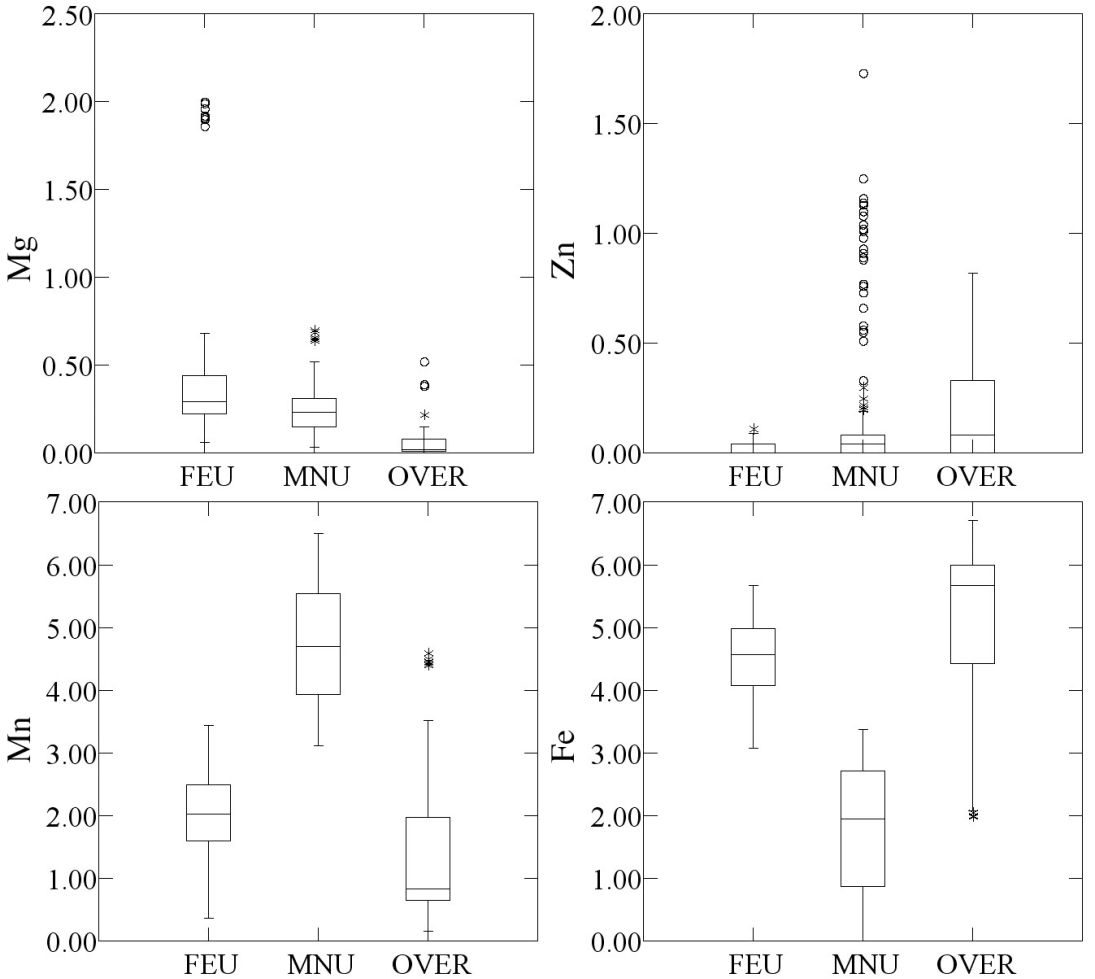

FIG. 9. Boxplots depicting the distribution of *O*-sheet cations (*apfu*) in astrophyllite-group minerals from silica undersaturated and silica-oversaturated intrusions. Paragenesis and boxplots are defined as in Figure 5.

crystal structure, limited substitution of Zr for Nb may be due to the significant (18%) difference in ionic radii between the cations ($r^{[6]}Ti^{4+}$: 0.61 Å, $r^{[6]}Nb^{5+}$: 0.64 Å, $r^{[6]}Zr^{4+}$: 0.72 Å, Shannon 1976). The crystal-chemical control on (Ti + Nb) ⇔ Zr and its effects on the *O* sheet will be presented in a future paper. Limited incorporation of Zr into the structure may also be the result of crystallization of environments depleted in Zr. It is of interest to note that in the petrological environments in which these minerals are found, the only commonly associated zirconosilicate is early-formed eudialyte; late-stage zirconosilicates characteristic of peralkaline environments, such as catapleiite, elpidite, gaidonnayite and lemoynite or natrolemoynite, are curiously absent, suggesting two phases of crystallization from geochemically distinct melts. The presence of limited Zr contents in astrophyllite-group minerals may be the result of alteration and mobilization of Zr from earlier Zr-bearing silicate minerals such as aegirine and amphiboles, whereas crystallization of late-stage zirconosilicates may require the introduction of a separate Zr-rich hydrothermal fluid.

Variations in Nb and Zr between environments are best represented by Nb – Zr *versus* Ti and Nb – Zr *versus* Mn#. As shown in Figures 12 and 13, kupletskite-subgroup samples (with the exception of four specimens from MSH) have strongly positive Nb – Zr values, indicating Nb > Zr. Astrophyllite-subgroup samples from undersaturated environments show negative values of Nb – Zr, indicating enrichment in Zr. Astrophyllite-

group minerals from oversaturated intrusions tend to have slightly positive Nb – Zr values, indicating slight enrichments in Nb over Zr. Such samples also have the lowest Zr contents (average: 0.20 *apfu*, range: 0.03 to 0.35 *apfu*). The lack of Zr in astrophyllite-group minerals from such oversaturated environments is directly related to the alkalinity and degree of SiO_2 saturation of the melt from which they crystallized. At an alkalinity index [AI = molar (Na + K)/Al] of 1.0 in SiO_2-saturated magmas, saturation in a Zr-bearing phase occurs early in the crystallization sequence, promoting early crystallization of zircon and inhibiting the formation of either Zr-rich alkali silicates. With increasing alkalinity and increased degree of undersaturation, alkali zirconosilicates are the dominant Zr-bearing minerals to form. Zirconium-poor astrophyllite containing inclusions of zircon have been noted from oversaturated dikes at Mount Rosa (Colorado) and on Kræmers Island (Kangerdlugssuaq, East Greenland; Layne *et al*. 1982), supporting this hypothesis.

The T sites

The dominant cation occupying all four unique *T* sites in minerals of this group is Si. Results from Mössbauer spectroscopy of many samples indicates the absence of $^{[4]}Fe^{3+}$. Similarly, site-scattering refinements of all four *T* sites during single-crystal X-ray refinements of the structure do not indicate significant departures from unity, implying the absence of any heavier

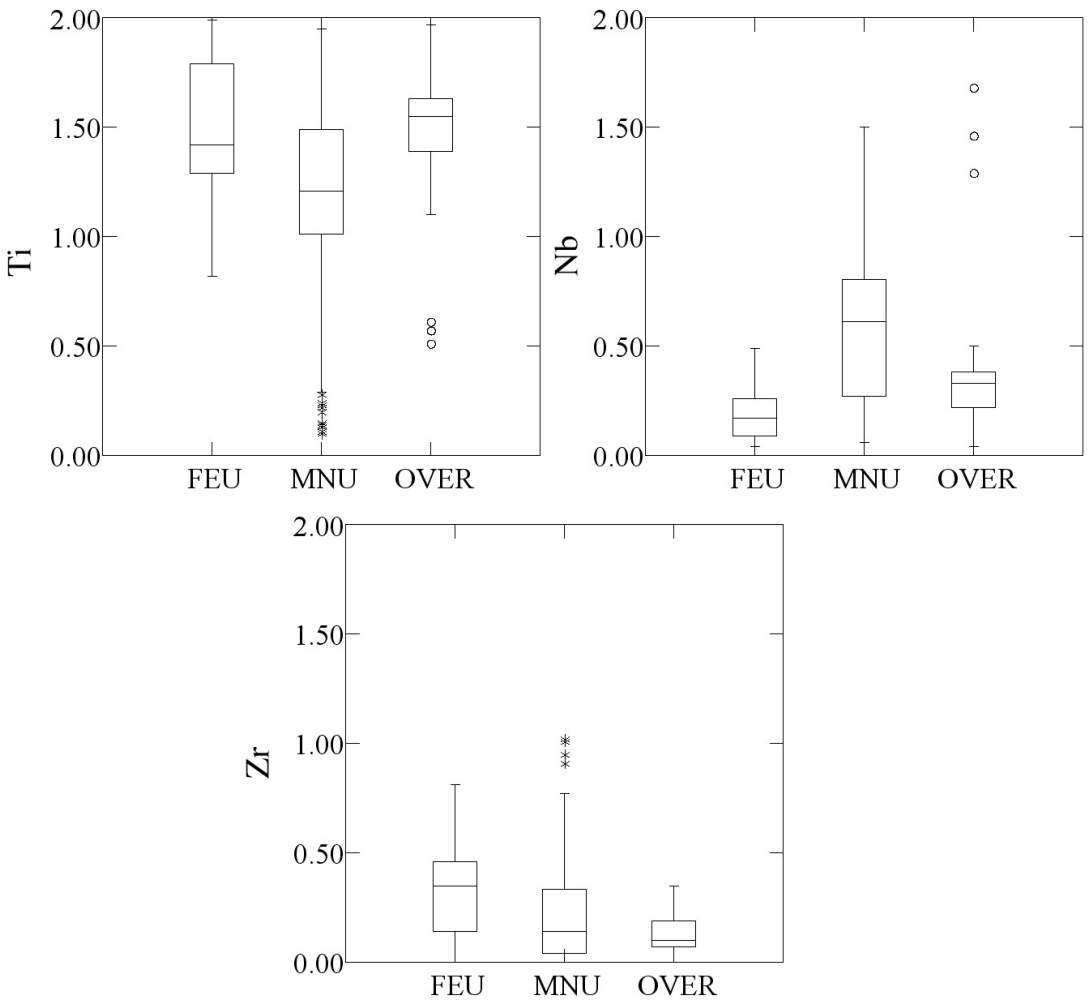

FIG. 10. Boxplots depicting the distribution of *D* cations (*apfu*) in astrophyllite-group minerals from silica-undersaturated and silica-oversaturated intrusions. Paragenesis and boxplots are defined as in Figure 5.

X-ray scatterers (*e.g.*, Ti, Fe^{3+}). Silicon contents range from 7.12 to 8.08 *apfu*, with Al ranging from below the detection limit to 0.73 *apfu*. As expected, a positive correlation exists between Si and Al (Fig. 14). Samples from oversaturated alkaline intrusions show the least extent of Al-for-Si substitution (average: 0.21 *apfu* Al), likely reflecting crystallization under SiO_2-enriched conditions, whereas kupletskite- and astrophyllite-subgroup samples from undersaturated environments show the greatest Al-for-Si substitution (average: 0.25 and

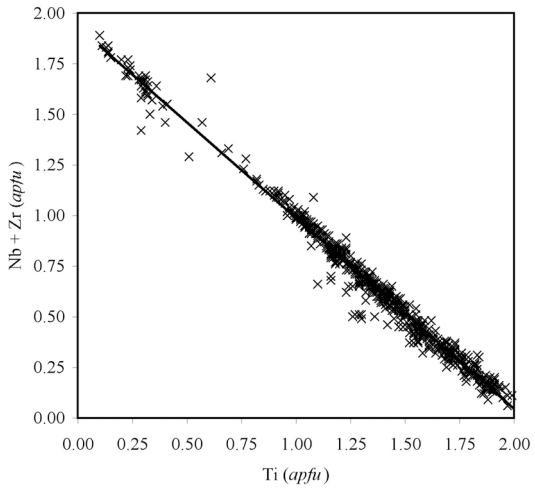

FIG. 11. The content of Ti *versus* that of (Nb + Zr) in *D* of astrophyllite-group minerals (linear regression: $R^2 = 0.986$, $n = 659$).

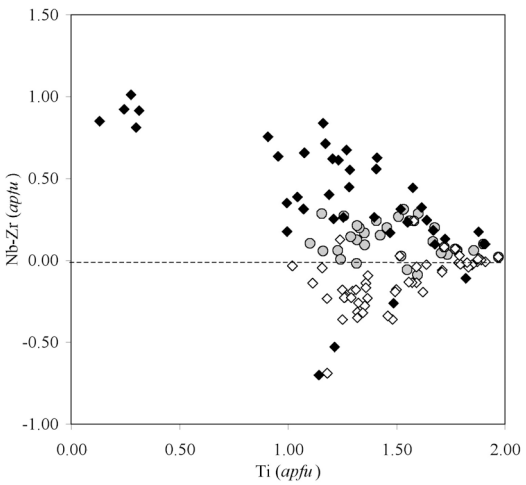

FIG. 12. The content of Ti *versus* (Nb – Zr) in *D* of astrophyllite-group minerals. Circles: OVER, closed diamonds: MNU, open diamonds: FEU. In general, MNU and OVER samples have Nb > Zr, whereas FEU samples have Zr > Nb.

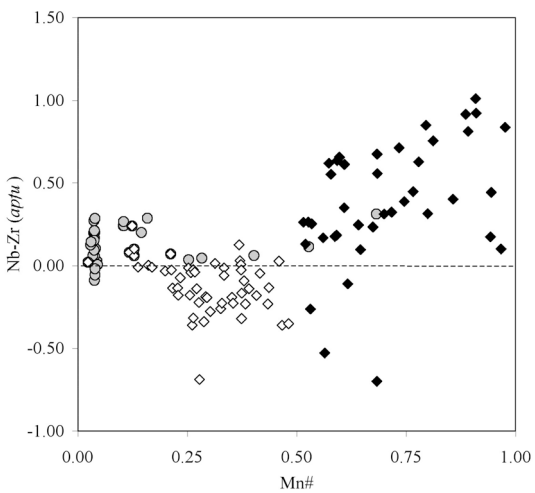

FIG. 13. Mn# *versus* (Nb – Zr) of astrophyllite-group minerals. Circles: OVER, closed diamonds: MNU, open diamonds: FEU. In general, MNU and OVER samples have Nb > Zr, whereas FEU samples have Zr > Nb.

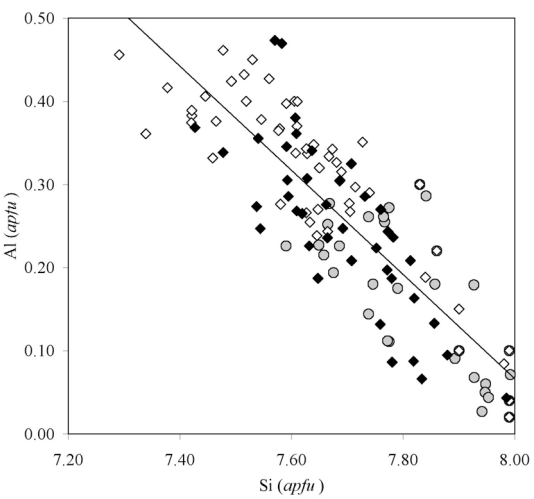

FIG. 14. The content of Si *versus* that of Al at the *T* sites in astrophyllite-group minerals. Circles: OVER, closed diamonds: MNU, open diamonds: FEU (linear regression: $R^2 = 0.745$).

0.32 *apfu* Al, respectively). In general, Al is a minor component in such minerals from both over- and undersaturated environments, perhaps the result of depletion of the melt in Al due to early crystallization of Al-bearing minerals such as sodalite and feldspathoids.

Substitutions and Solid-Solution Series in the Astrophyllite-Group

In light of the chemical variations described above, solid-solution series have been confirmed, either wholly or in part, between the following pairs of astrophyllite-group minerals.

1. astrophyllite – kupletskite (complete, $Fe^{2+} \Leftrightarrow Mn$)
2. kupletskite – niobokupletskite (complete, Ti + F $\Leftrightarrow$ Nb + O)
3. astrophyllite – niobophyllite (partial, Ti + F $\Leftrightarrow$ Nb + O)
4. kupletskite – zircophyllite (partial, Ti $\Leftrightarrow$ Zr)
5. astrophyllite– Fe-dominant analogue of zircophyllite (partial, Ti $\Leftrightarrow$ Zr).

The dominant mehanisms of substitution observed in the samples studied are outlined in Table 6. The most complex of the solid solutions involves species in which Nb is incorporated into the astrophyllite-group structure. Incorporation of a pentavalent cation at *D* requires a number of considerations with respect to charge balance. Abdel-Rahman (1992) suggested that Nb enters the structure *via* the substitution Nb $\Leftrightarrow$ Ti + $\square$, and Birkett *et al*. (1996) subsequently suggested the coupled substitutions Nb + $Fe^{3+} \Leftrightarrow 2R^{4+}$ and Nb + $(Mn,Fe)^{2+} \Leftrightarrow 3Ti^{4+}$. Problems with the proposed schemes include the absence of charge balance, the creation of vacancies, and the incorporation of Fe^{2+} and Fe^{3+} at *D*, all features that are not supported by the EMPA data, single-crystal X-ray refinements of the structure and Mössbauer spectroscopy.

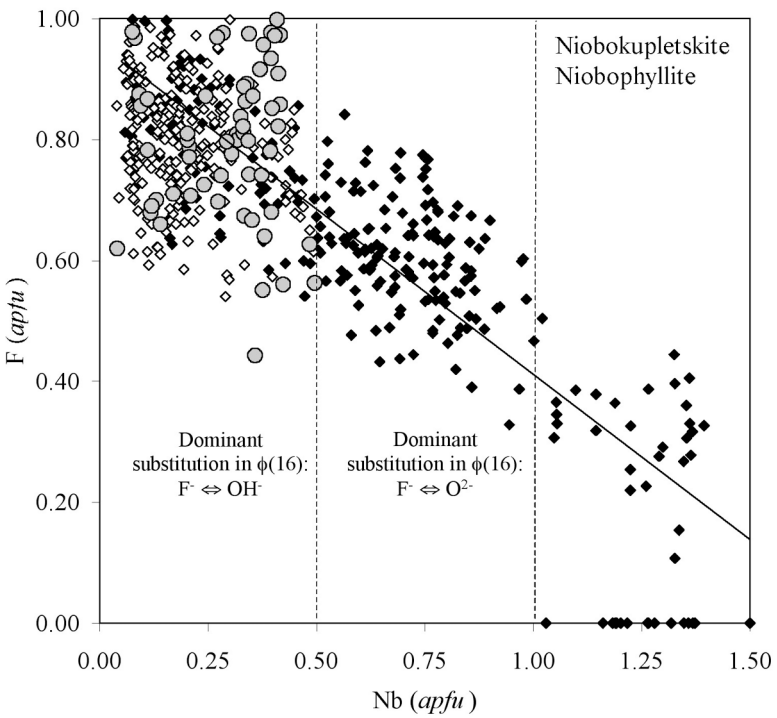

FIG. 15. Content of Nb *versus* that of F in astrophyllite-group minerals. Substitution of Nb into the structure occurs in niobokupletskite, niobophyllite and Nb-bearing kupletskite as the result of the substitution Ti + F = Nb + O. Samples of the astrophyllite subgroup and those from oversaturated rocks do not show significant enrichment in Nb and can therefore be expressed by the substitution Ti + F $\Leftrightarrow$ Zr + (F,OH). In MNU samples, Nb = 0.50 *apfu* represents the limiting value at which these two mechanisms of substitution exchange dominance in the structure. The regression line (R^2 = 0.7601) demonstrates the strong negative correlation between Nb and F only in kupletskite-subgroup samples. Circles: OVER, open diamonds: MNU, closed diamonds: FEU.

Incorporation of Nb^{5+} into the structure in nioboku-pletskite, niobophyllite and Nb-bearing kupletskite is best modeled by the coupled substitution Ti + F ⇔ Nb + O (Piilonen *et al.* 2000). In astrophyllite-subgroup samples, the proportion of Zr exceeds that of Nb, and the dominant mechanism of substitution involves Zr and not Nb, which can thus be expressed as Ti + F ⇔ Zr + (F,OH). When calculation of the general formula was discussed in earlier sections, we showed that Nb = 0.50 a*pfu* is used as a limiting value to determine the preferred method to calculate the formula of an astrophyllite-group mineral. This value seems to represent a limiting value at which the two mechanisms of substitution above exchange dominance in the structure (Fig. 15).

Incorporation of Nb into the astrophyllite structure is facilitated by oxidizing conditions in the melt from which minerals of this group crystallized. This oxidation of the melt also results in increased $Fe^{3+} \Leftrightarrow M^{2+}$ substitution in the *O* sheet. To maintain charge balance, the incorporation of Fe^{3+} must also be accompanied by substitution of Na for M^{2+}, which has been shown by single-crystal X-ray structure refinements to occur at *M*(1). The Fe^{3+} must therefore be incorporated either at *M*(2) or *M*(3) in order to satisfy the bond-valence requirements of the O(2) oxygen, to which *M*(1), *M*(2), *M*(3) and *D* are bonded. As such, a more complex scheme of substitution has been developed for Nb-rich samples, incorporating Fe^{3+} contents derived from Mössbauer spectroscopy (Fig. 16):

$$M(1)^{2+} + M(2,3)^{2+} + (Zr,Ti) + F \Leftrightarrow {}^{M(1)}Na + {}^{M(2,3)}Fe^{3+} + Nb + O \quad (7).$$

Summary

Members of the astrophyllite group display a wide range of chemical compositions, the result of having a complex and accommodating structure, with a variety of sites at which substitutions may take place. The proposed general formula has been developed taking into consideration the wide range of isomorphous substitutions possible, and under the assumption that new species will be discovered in the future. Although a complete crystal-chemical description of any member of the astrophyllite group requires both detailed chemical data and a single-crystal X-ray determination of its structure, we can make a number of generalizations about astrophyllite-group minerals:

1) The standardized general formula for all members of the astrophyllite group can be written as $A_2BC_7D_2T_8O_{26}(OH)_4X_{0-1}$, where $^{[10]-[13]}A$ = K, Rb, Cs, H_3O^+, H_2O, Na or □; $^{[10]}B$ = Na or Ca; $^{[6]}C$ = Mn, Fe^{2+}, Fe^{3+}, Na, Mg, or Zn; D = $^{[6]}$Ti, Nb, or Zr; $^{[4]}T$ = Si or Al, X = ϕ = F, OH, O, or □.

2) Calculation of the formula of members of the group with >5.00 wt.% Nb_2O_5 is best based on 26O + 4(OH) + (F,O). For those with <5.00 wt.% Nb_2O_5, the calculation is best based on 26O + 5(OH,F). Formula calculation for magnesium astrophyllite is best based on 26O and 4(OH,F).

3) We have shown that F orders preferentially at ϕ(16), the bridging anion position between $D\phi_6$ octahedra, and not into the two monovalent anion sites located in the O sheet [OH(4) and OH(5)].

4) The interlayer in all minerals of this group is dominated by $^{[13]}$K and $^{[10]}$Na. Other elements to be incorporated in *A* and *B* include Rb, Cs, Sr, Ba, H_2O and Ca. No evidence for H_3O^+ exists in the suite of samples studied. No mineral studied contains essential Li.

5) The dominant mechanism of substitution in the *O* sheet is Mn ⇔ Fe^{2+}, resulting in complete solid-solution between astrophyllite- and kupletskite-subgroup

TABLE 6. POSSIBLE MECHANISMS OF SUBSTITUTION IN MINERALS OF THE ASTROPHYLLITE GROUP

Substitution	Site at which substitution occurs	Exchange operators
K ⇔ (Cs,Rb)	$^{[13]}A$	$K(Cs,Rb)_{-1}$
Na + Si ⇔ Ca + Al	$^{[10]}B$, $^{[4]}T$	$NaSi(CaAl)_{-1}$
K ⇔ Na	$^{[13]}A$	KNa_{-1}
Mn ⇔ Fe^{2+}	$^{[6]}M$	$MnFe^{2+}_{-1}$
Zn ⇔ Fe^{2+}	$^{[6]}M(2,3,4)$	$ZnFe^{2+}_{-1}$
Zn ⇔ Mn	$^{[6]}M(2,3,4)$	$ZnMn_{-1}$
Mg ⇔ Fe^{2+}	$^{[6]}M(2,3,4)$	$MgFe^{2+}_{-1}$
Mg ⇔ Mn	$^{[6]}M(2,3,4)$	$MgMn_{-1}$
Na ⇔ Mn	$^{[6]}M(1)$	$NaMn_{-1}$
Zr ⇔ Ti	$^{[6]}D$	$ZrTi_{-1}$
Nb + O ⇔ Ti + F	$^{[6]}D$, ϕ(16)	$NbO(TiF)_{-1}$
$M(1,2,3)^{2+}$ + (Zr,Ti) + F ⇔ $^{M(1)}Na + {}^{M(2,3)}Fe^{3+}$ + Nb + O	$^{[6]}M(1,2,3)$, $^{[6]}D$, ϕ(16)	$M^{2+}(Zr,Ti)F(NaFe^{3+}NbO)_{-1}$

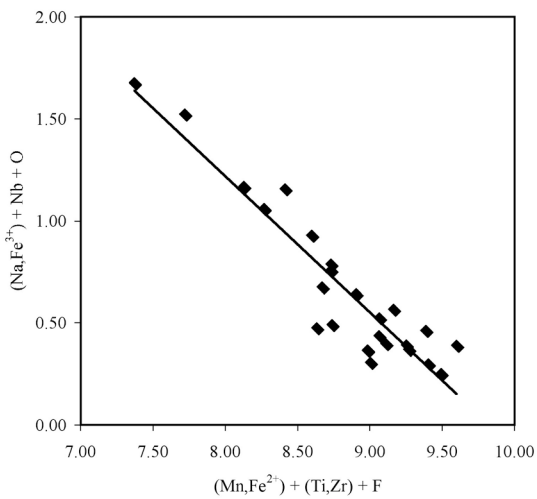

FIG. 16. Mechanism of substitution for the incorporation of Nb^{5+} into the structure: $M^{2+} + M^{4+} + F^- \Leftrightarrow (Na,Fe^{3+}) + Nb^{5+} + O^{2-}$ (linear regression, $R^2 = 0.870$).

species. Results from Mössbauer spectroscopy indicate Fe^{3+}/Fe_{tot} values in the range from 0.01 to 0.21, corresponding to 0.05 to 0.56 *apfu* Fe^{3+}, confirming that Fe^{2+} is the dominant valence state of iron in the structure. Both Fe^{2+} and Fe^{3+} are restricted to the *O* sheet. Other cations present in the *O* sheet include Na (up to 0.43 *apfu*), Mg and Zn.

6) The *D* site is dominated by Ti, Zr and Nb, with trace concentrations of Hf (up to 0.04 *apfu*) and Ta (up to 0.13 *apfu*). Substitution of Nb for Ti appears to be extensive (84% solid solution), resulting in both niobokupletskite and niobophyllite. The incorporation of Nb into the structure is the result of a coupled substitution, Ti + F ⇔ Nb + O. Substitution of Zr for Ti appears to be limited (51% solid solution), resulting in both zircophyllite and a potentially new mineral, the Fe-dominant analogue of zircophyllite.

7) Aluminum is a minor component of the structure; substitution of Al for Si in the *T* sites ranges from zero to 0.47 *apfu*. There is no evidence of $^{[4]}Fe^{3+}$.

8) The principal substitutions in the astrophyllite-group include K ⇔ (Cs,Rb), Si + Na ⇔ Al + Ca, Ti = Nb, Ti ⇔ Zr, Mn ⇔ Fe^{2+}, (Mg,Zn) ⇔ (Mn,Fe^{2+}) and (Mn,Fe) ⇔ Na.

9) Astrophyllite-group minerals from silica-oversaturated intrusions show enrichments in Rb, Fe^{2+}, Ti, Si and F. Kupletskite-subgroup samples from silica-undersaturated intrusions show enrichments in Na, Mn, Fe^{3+}, Zn, Zr and Nb, whereas astrophyllite-subgroup samples from silica-undersaturated intrusions show enrichments in K, Ca, Fe^{2+}, Ti, Zr and Al.

Acknowledgements

The authors thank Mr. M.A. Cooper and Dr. F.C. Hawthorne (Department of Geological Sciences, University of Manitoba) and Dr. G. Yap (Dept. of Chemistry, University of Ottawa), for use of the CCD diffractometer, Mrs. E. Moffatt (Canadian Conservation Institute) for performing the IR analyses, Dr. D.J. Cherniak (Department of Earth and Environmental Sciences, Rensselaer Polytechnic Institute) for the NRA analyses, and to Dr. D.G. Rancourt (Department of Physics, University of Ottawa) for use of the Mössbauer spectrometer. This study would not have been possible without the generous donation of samples from a number of institutions and mineral collectors. Special thanks are extended to the Fersman Mineralogical Museum (Moscow, Russia), the Royal Ontario Museum (Toronto, Canada), the Geological Survey of Canada (Ottawa, Canada), Mineralogisk-Geologisk Museum (University of Oslo, Norway), P. Tarassoff, Q. Wight, L. Horváth, R. Werner, O.V. Petersen, D. Belakovskiy, K. Day, M. Webber, C.C. Christiansen, H. DeLinde, T. Birkett, S. Szilard, S. Dahlgren and A.-F. Abdel-Rahman. The comments by two referees, Drs. I.V. Pekov and B. Grobéty, as well as by Associate Editor O. Johnsen and R.F. Martin, are greatly appreciated. Financial support was provided by the Natural Sciences and Engineering Research Council of Canada in the form of a scholarship to PCP and grants to AEL and AMM, and by the University of Ottawa and Laurentian University.

References

Abdel-Rahman, A.F.M. (1992): Mineral chemistry and paragenesis of astrophyllite from Egypt. *Mineral. Mag.* **56**, 17-26.

Aja, S.U., Wood, S.A. & Williams-Jones, A.E. (1995): The aqueous geochemistry of Zr and the solubility of some Zr-bearing minerals. *Appl. Geochem.* **10**, 603-620.

Birkett, T.C., Trzcienski, W.E. & Stirling, J.A.R. (1996): Occurrence and compositions of some Ti-bearing minerals in the Strange Lake intrusive complex, Québec–Labrador boundary. *Can. Mineral.* **34**, 779-801.

Brøgger, W.C. (1890): Die Mineralien der Syenitpegmatitgänge der südnorwegischen Augit- und Nephelinsyenite. *Z. Kryst. Mineral.* **16**, 1-235, 1-663.

Chelishchev, N.F. (1972): Ion exchange properties of astrophyllites under supercritical conditions. *Geochem.* **7**, 856-860.

Christiansen, C.C. (1998): *Mineralogisk, krystalkemisk og krystallografisk undersøgelse af astrophylitgruppens medlemmer fra mineralforekomster i Grønland*. M.Sc. thesis, Univ. Copenhagen, Copenhagen, Denmark.

_____, Johnsen, O. & Ståhl, K. (1998): Crystal structure of kupletskite from the Kangerdlugssuaq intrusion, East Greenland. *Neues Jahrb. Mineral. Monatsh.*, 253-264.

Cohen, B.L., Fink, C.L. & Degnan, J.H. (1972): Nondestructive analysis for trace amounts of hydrogen. *J. Appl. Phys.* **43** 19-25.

Crerar, D., Wood, S., Brantley, S. & Bocarsly, A. (1985): Chemical controls on solubility of ore-forming minerals in hydrothermal systems. *Can. Mineral.* **23**, 333-352.

Czamanske, G.K. & Mihálik, P. (1972): Oxidation during magmatic differentiation, Finnmarka Complex, Oslo area, Norway. 1. The opaque oxides. *J. Petrol.* **13**, 493-509.

_____ & Wones, D.R. (1973): Oxidation during magmatic differentiation, Finnmarka Complex, Oslo area, Norway. 2. The mafic silicates. *J. Petrol.* **14**, 349-380.

Efimov, A.F., Dusmatov, V.D., Ganzeev, A.A. & Kataeva, Z.T. (1971): Cesium kupletskite, a new mineral. *Dokl. Acad. Sci. USSR, Earth Sci. Sect.* **197**, 140-143.

Farmer, V.C. (1974): Infrared Spectra of Minerals. *Mineral. Soc., Monogr.* **4**.

GANZEYEV, A.A., YEFIMOV, A.F.& SEMENOVA, N.G. (1969): Isomorphism of the alkali metals in minerals of the astrophyllite-group. *Geochem. Int.* **6**, 295-300.

HAWTHORNE, F.C., OBERTI, R., CANNILLO, E., OTTOLINI, L., ROELOFSEN, J.N. & MARTIN, R.F. (2001): Li-bearing arfvedsonitic amphiboles from the Strange Lake peralkaline granite, Québec. *Can. Mineral.* **39**, 1161-1170.

_____, UNGARETTI, L., OBERTI, R., BOTTAZZI, P. & CZAMANSKE, G.K. (1993): Li, an important component in igneous alkali amphiboles. *Am. Mineral.* **78**, 733-745.

_____, _____, _____, CANNILLO, E. & SMELIK, E.A. (1994): The mechanism of $^{[6]}$Li incorporation in amphiboles. *Am. Mineral.* **79**, 443-451.

HUBEI GEOLOGIC COLLEGE, X-RAY LABORATORY (1974): The crystal chemistry of astrophyllite-group minerals. *Sci. Geol. Sinica* **1**, 18-33 (in Chinese).

JOHNSEN, O. & GAULT, R.A. (1997): Chemical variation in eudialyte. *Neues Jahrb. Mineral., Abh.* **171**, 215-237.

KAPUSTIN, YU.L. (1973): Zircophyllite, the zirconium analogue of astrophyllite. *Int. Geol. Rev.* **15**, 621-625.

KRAUSKOPF, K.B. (1967): *Introduction to Geochemistry*. McGraw-Hill, New York, N.Y.

LALONDE, A.E., RANCOURT, D.G. & CHAO, G.Y. (1996): Fe-bearing trioctahedral micas from Mont Saint-Hilaire, Québec, Canada. *Mineral. Mag.* **60**, 447-460.

LANFORD, W.A. (1992): Analysis for hydrogen by nuclear reaction and energy recoil detection. *Nucl. Instrum. Methods Phys. Res.* **B66**, 65-82.

LAYNE, G.D., RUCKLIDGE, J.C.& BROOKS, C.K. (1982): Astrophyllite from Kangerdlugssuaq, East Greenland. *Mineral. Mag.* **45**, 149-156.

LIEBAU, F. (1985): *Structural Chemistry of Silicates: Structure, Bonding and Classification*. Springer-Verlag, Berlin, Germany.

MACDONALD, R. & SAUNDERS, M.J. (1973): Chemical variation in minerals of the astrophyllite-group. *Mineral. Mag.* **39**, 97-111.

MANNING, P.G. (1969): On the origin of colour and pleochroism of astrophyllite and brown clintonite. *Can. Mineral.* **9**, 663-677.

MARTIN, D. (1975): *Studies of Astrophyllite from Mont Saint-Hilaire*. B.Sc. thesis, Carleton Univ., Ottawa, Canada.

MASON, R.A. (1992): Models of order and iron–fluorine avoidance in biotite. *Can. Mineral.* **30**, 343-354.

MCAULIFFE, C.A. & BARRATT, D.S. (1987): Titanium. *In* Comprehensive Coordination Chemistry. **3**. Main Group and Early Transition Elements (G. Wilkinson, R.D. Gillard & J.A. McCleverty, eds.). Pergamon, Oxford, U.K. (323-362).

MUNOZ, J.L. (1984): F–OH and Cl–OH exchange in micas with applications to hydrothermal ore deposits. *In* Micas (S.W. Bailey, ed.). *Rev. Mineral.* **13**, 469-493.

_____ & LUDINGTON, S.D. (1974): Fluoride–hydroxyl exchange in biotite. *Am. J. Sci.* **274**, 396-413.

NICKEL, E.H., ROWLAND, J.F. & CHARETTE, D.J. (1964): Niobophyllite – the niobium analogue of astrophyllite; a new mineral from Seal Lake, Labrador. *Can. Mineral.* **8**, 40-52.

NIELSEN, C.H. & SIGURDSSON, H. (1981): Quantitative methods for electron microprobe analysis of sodium in natural and synthetic glasses. *Am. Mineral.* **66**, 547-552.

PENG, C.C. & MA, C.S. (1963): Crystal structure of astrophyllite and a new type of band silicate radical. *Sci. Sinica* **12**, 272-276 (in Chinese).

PIILONEN, P.C., LALONDE, A.E., MCDONALD, A.M. & GAULT, R.A. (2000): Niobokupletskite, a new astrophyllite-group mineral from Mont Saint-Hilaire, Québec: description and crystal structure. *Can. Mineral.* **38**, 627-639.

_____, MCDONALD, A.M. & LALONDE, A.E. (2001): Kupletskite polytypes from the Lovozero massif, Kola Peninsula, Russia: kupletskite-1*A* and kupletskite-*Ma2b2c*. *Eur. J. Mineral.* **13**, 973-984.

_____, _____ & _____ (2003): Insight into astrophyllite-group minerals. II. Crystal chemistry. *Can. Mineral.* **41**, 27-54.

RANCOURT, D.G., DANG, M.-Z. & LALONDE, A.E. (1992): Mössbauer spectroscopy of tetrahedral Fe^{3+} in trioctahedral micas. *Am. Mineral.* **77**, 34-43.

_____, PING, J.Y., BOUKILI, B. & ROBERT, J.-L. (1996): Octahedral-site Fe^{2+} quadrupole splitting distributions from Mössbauer spectroscopy along the (OH,F)-annite join. *Phys. Chem. Minerals* **23**, 63-71.

SALVI, S., FONTAN, F., MONCHOUX, P., WILLIAMS-JONES, A.E. & MOINE, B. (2000): Hydrothermal mobilization of high field strength elements in alkaline igneous systems: evidence from the Tamazeght complex (Morocco). *Econ. Geol.* **95**, 559-576.

_____ & WILLIAMS-JONES, A.E. (1995): Zirconosilicate phase relations in the Strange Lake (Lac Brisson) pluton, Québec–Labrador, Canada. *Am. Mineral.* **80**, 1031-1040.

SCHEERER, T. (1854): Verhandlungen des bergmännischen vereins zu Freiberg. *Berg Hütten. Zeitung* **12**, 389-392.

SEMENOV, E.I. (1956): Kupletskite, a new mineral of the astrophyllite group. *Dokl. Akad. Nauk SSSR* **108**, 933-936.

SHABANI, A.A.T. (1999): *Mineral Chemistry and Mössbauer Spectroscopy of Micas from Granitic Rocks of the Canadian Appalachians*. Ph.D. thesis, Univ. Ottawa, Ottawa, Canada.

SHANNON, R.D. (1976): Revised effective ionic radii and systematic studies of interatomic distances in halides and chalcogenides. *Acta Crystallogr*. **A32**, 751-767.

SHI, NICHENG., MA, ZHESHENG, LI, GUOWU, YAMNOVA, N.A. & PUSHCHAROVSKY, D.YU. (1998): Structure refinement of monoclinic astrophyllite. *Acta Crystallogr*. B**54**, 109-114.

SPRAY, J.G. & RAE, D.A. (1995): Quantitative electron-microprobe analysis of alkali silicate glasses: a review and user guide. *Can. Mineral*. **33**, 323-332.

WEIBYE, P.C. (1848): Beiträge zur topographischen Mineralogie Norwegens. *Archib für Mineralogie, Geognosie Bergbau und Hüttenkunde* **22**, 465-544.

WOODROW, P.J. (1967): The crystal structure of astrophyllite. *Acta Crystallogr.* **22**, 673-678.

Received February 17, 2002, revised manuscript accepted December 28, 2002.